Title
Nano fabrication approaches for patterned magnetic recording media

Author
Choi, Chulmin

Publication Date
2010

Peer reviewed|Thesis/dissertation

UNIVERSITY OF CALIFORNIA, SAN DIEGO

Nano Fabrication Approaches for Patterned Magnetic Recording Media

A dissertation submitted in partial satisfaction of the

requirements for the degree Doctor of Philosophy

in

Materials Science and Engineering

by

Chulmin Choi

Committee in Charge:

Professor Sungho Jin, Chair
Professor Prabhakar Bandaru
Professor Jennifer Cha
Professor Vlado A. Lubarda
Professor Yu Qiao

2010

The dissertation of Chulmin Choi is approved, and it is acceptable in quality and form for publication on microfilm:

Chair

University of California, San Diego

2010

Dedicated to

my wife, Hannah

“You will know the truth, and the truth will set you free.”

John 8:32

TABLE OF CONTENTS

LIST OF FIGURES

LIST OF TABLES

ACKNOWLEDGEMENTS

I wish to acknowledge and deeply thank my advisors, Professor Sungho Jin for his strong encouragement, support, and guidance during the course of this research. I wish to express my gratefulness to my committee members for their time and helpful suggestions: Professor Prabhakar Bandaru, Professor Yu Qiao, Professor Valdo A. Lubarda, and Professor Jennifer Cha.

Chapter 3, in full, has been prepared for a manuscript for publication, “Planarization of Patterned Magnetic Recording Media to Enable Head Flyability”, (In preparation) by Chulmin Choi, Yeoungchin Yoon, Daehoon Hong, Young Oh, Frank E. Talke and Sungho Jin. Chapter 4, in full, has been prepared for a manuscript for publication, “Enhanced Magnetic Properties of Bit Patterned Magnetic Recording Media by Trench-Filled Nanostructure”, Chulmin Choi, Daehoon Hong, Young Oh, Leon Chen, Sy-Hwang Liou and Sungho Jin

I would also like to recognize and thank the following individuals for their assistance in various aspects of this work: Dr. Daehoon Hong, Dr. Leon Chen, Yeoungchin Yoon, Kunbae Noh, Young Oh, Jinyeol Kim and Karla Brammer. I appreciate all the helps from my collaborators. We have shared the joy and frustration together solving countless materials, fabrications and device problems in the past several years.

I wish to thank Nano3 staffs at UC San Diego: Dr. Bernd Fruhberger, Larry Grissom, Ryan Anderson, Dr. Maribel Montero, and Sean Parks. They have been always ready to help with the nanofabrication and characterization processes.

I would like to thank CNST staffs of National Institute of Standards and Technology (NIST): Dr. Lei Chen, Richard Kasica, and Jeff Pasternak. I certainly appreciate their helping me out in lithography processes. The assistance in micro MOKE (magneto-optical Kerr Effect) measurements of geometry-altered magnetic island samples by Prof. Eric Fullerton of CMRR (Center for Magnetic Recording Research) and ECE Department and Dr. Olav Hellwig of Hitachi Global Storage Technology is also acknowledged.

Special thanks go to Charlotte Lauve, Betty Manoulian, and Iris Villanueva for taking care of the administrative burdens for me.

Finally, I wish to thank my wife and other family members for their prayers and loving encouragement during this time. Thanks again to my wife, Hannah Lim, for her best support for my effort toward the PhD degree.

I also wish to thank my many friends and other colleagues who are too numerous to mention all by name.

Chulmin Choi

La Jolla, June 2010

VITA

1976	Born in Seoul, South Korea
2002	B.S., Material Science and Engineering, University of Incheon, Incheon, South Korea
2004	M.S., Material Science and Engineering, Korea University, Seoul, South Korea
2005	Samsung Advanced Institute of Technology Hard Disk Drive Team, Suwon, South Korea
2010	Ph.D., Materials Science and Engineering, University of California, San Diego

SELECTED AWARDS

Awarded with Sheldon Schultz Prize for Excellence in Graduate Student Research, 2010

Awarded with the Materials Science Research Assistant Fellowship,
University of California, San Diego for the year 2007-2010

Awarded with the UCSD Chancellor Fellowship for Graduate Student ,
University of California, San Diego for the year 2006-2007.

Awarded with the Graduate Study Abroad Scholarship by the Korean Science and Engineering Foundation (KOSEF) for the year 2005-2006.

Awarded with the National Research Lab (NRL) Scholarship,
Korea University Seoul, Korea for the year 2001-2002.

PUBLICATIONS

Journals Articles:

1. “Enhanced Magnetic Properties of Bit Patterned Magnetic Recording Media by Trench-Filled Nanostructure”, Chulmin Choi, Daehoon Hong, Young Oh, Leon Chen, Sy-Hwang Liou and Sungho Jin, J. Vac. Sci. Technol. B. (in press)
2. “Optically transparent glass with vertically aligned surface Al_2O_3 nanowires having superhydrophobic characteristics” Nano (in press)
3. “Strongly Superhydrophobic Silicon Nanowires by Supercritical CO_2 Drying”, Chulmin Choi, Yeoungchin Yoon, Daehoon Hong, Karla S. Brammer, Kunbae Noh, Young Oh, Seunghan Oh, Frank E. Talke and Sungho Jin, Electronic Materials Letters (in press)
4. “Planarization of Discrete Track Recording Media to Improve Flyability of Magnetic Recording Sliders”, Yoon, Y.; Choi, C.; Oh, Y.; Hong, D.; Jin, S.; Talke, F.E.; IEEE Trans. Mag., 45(10), 3527 (2009)
5. “Antibiofouling, Sustained Antibiotic Release by Si Nanowire Templates”, Karla S. Brammer, Chulmin Choi, Seunghan Oh, Christine J. Cobb, Laura S. Connelly, Mariana Loya, Seong Deok Kong, and Sungho Jin, Nano Lett., 9(10), 3570 (2009)
6. “50 nm DNA Nanoarrays Generated from Uniform Oligonucleotide Films", Hyunwoo Noh, Albert M. Hung, Chulmin Choi, Ju Hun Lee, Jin-Yeol Kim, Sungho Jin, and Jennifer N. Cha, ACS Nano, 3(8), 2376 (2009)
7. “Geometry transformation and alterations of periodically patterned Si nanotemplates by dry oxidation”, Jeongwon Park, Li-Han Chen, Daehoon Hong, Chulmin Choi, Mariana Loya, Karla Brammer, Prab Bandaru, and Sungho Jin, Nanotechnology, 20, 015303 (2009)
8. “Control of M-H Loop Shape in Perpendicular Recording Media By Ion Implantation”, Chulmin Choi, Daehoon Hong, Andrew I. Gapin, and Sungho Jin, IEEE Trans. Mag., 43(6), 2121 (2007)
9. "Thermal stability of magnetic tunnel junctions with new amorphous ZrAl alloy films as the under and cappin layers", Chulmin Choi, Jinoh Song, and Seongrae Lee, IEEE Trans. Mag., 41, 2667 (2005)
10. “Thermal and electrical stability behavior of the magnetic tunnel junction with a new Zr-alloyed Al-oxide barrier ”, Chul-Min Choi and Seong-Rae Lee, IEEE Trans. Mag., 40(4), 2281 (2004)
11. "Influence of insulating barrier tickness in the magnetoresistance properties of the magnetic tunnel junction with Zr-alloyed Al-oxide barrier", Chul-Min Choi and Seong-Rae Lee, phys. stat. sol.(a) 201, 1704 (2004)
12. “Surface roughness effects of bias voltage characteristics in CoNbZr-based magnetic tunnel junction”, B. S. Chun, C. -M. Choi, I. C. Chu, S.-R. Lee, and Y. K. Kim, J. Magn. Magn. Mater. 272~276, E1481 (2004)
13. “Effect of Zr concentration on the microstructure of Al and the magnetoresistance properties of the magnetic tunnel junction with a Zr-alloyed Al-oxide barrier”,

Seong-Rae Lee, Chul-Min Choi, and Young Keun Kim, Appl. Phys. Lett. 83(2), 317 (2003)

Patents / Technology disclosures:

1. Jennifer N. Cha, Hyunwoo Noh, Sungho Jin, Chulmin(Edward) Choi, Jin Yeol Kim, and Albert Hung, "Geometry-Defined Surface Confined Diffusion And Orthogonal DNA Interactions To Obtain Long-Range Order In Nanoparticle Arrays" (UCSD Docket No.SD2009-274-2)
2. Sungho Jin, Chulmin Choi, Jin-Yeol Kim, and Kunbae Noh, "Self-Cleaning, Superhydrophobic Coatings with Improved Properties, Methods for Fabrication, and Applications Thereof" (UCSD Docket No. SD2009-035)
3. Sungho Jin, Daehoon Hong, Chulmin Choi, "Novel and Convenient Single CD Probe and Arrayed Nano Probes Fabricated by Using Chemical Etching of Nano-Hole-Array Patterned Substrate, and Applications Using Such Probes" (UCSD Docket No. SD2009-042)
4. Sungho Jin, Daehoon Hong, Chulmin Choi, "Planarization of Three-Dimensional Micro and Nano Devices (UCSD Docket No. SD2009-175)
5. Sungho Jin, Karla Brammer, Chulmin Choi, "Anti-Biofouling, Implant and Drug Release Devices by Nanowire Structures Comprising Si, Fabrication Method, and Biomedical Uses" (UCSD Docket No. SD2010-013)
6. Sungho Jin, Daehoon Hong, Chulmin Choi, Young Oh, "Article Comprising Thin Sliced Semiconductors by Magnetic-Field-Guided Etching, Method of Slicing, and Device Applications (UCSD Docket No. SD2010-071)
7. Hoonsang Oh, Hoosan Lee, Chulmin Choi, Youngsoo Kim, Noyeol Park, "Perpendicular magnetic recording media with softmagnetic underlayer", Korea Patent 10-2005-0058643
8. Seong-Rae Lee, Chul-Min Choi, JinOh Song,"Multilayer structure of Device using Ti_xAl_{1-x} ($0<x<1$) as underlayer or cappinglayer", Korea Patent 10-2005-0036520
9. Seong-Rae Lee, Chul-Min Choi, "Magnetoresistance device", USA Patent 10/765,970, January 29 (2004)
10. Seong-Rae Lee, Chul-Min Choi, JinOh Song, SungMin Park, "Magnetoresistance device and manufacturing method thereof", Korea Patent 10-2004-0003812
11. Seong-Rae Lee, Chul-Min Choi, JinOh Song, SungMin Park, "Magnetoresistance device and manufacturing method thereof", Korea Patent 10-2004-0003811
12. Seong-Rae Lee, Chul-Min Choi, Jong-Soo Kim, and Donghwan Kim "Multilayer Device using ZrAlOx under capping layer", Korea Patent 10-2003-0069701
13. Seong-Rae Lee, Chul-Min Choi, Jong-Soo Kim, and Donghwan Kim "Multilayer Device using ZrAl under capping layer", Korea Patent 10-2003-0069700
14. Seong-Rae Lee and Chul-Min Choi, "Tunneling magnetoresistance device and method of manufacturing the same", Korea Patent 10-2003-0005915

Proceedings and Conference Presentation:

1. “Patterned Magnetic Recording Media – Topography and Magnetic Properties”, Chulmin Choi, Daehoon Hong, Young Oh, Mariana Loya, Li-Han Chen and Sungho Jin, 2009 Materials Research Society Fall meeting, December (2009)
2. “Long-Range Ordered Aluminum Oxide Nanotubes by Guided Anodization”, Kunbae Noh, Chulmin Choi, Jin-Yeol Kim, Mariana Loya and Sungho Jin, 2009 Materials Research Society Fall meeting, December (2009)
3. “Topography and magnetic properties of planarized patterned magnetic recording media”, Chulmin Choi, Young Oh, Mariana Loya, Daehoon Hong and Sungho Jin, IEEE International Magnetics Conference, May (2009)
4. “Planarization of discrete track recording media to improve flyability of magnetic recording sliders”, Yeongchin Yoon, Chulmin Choi, Young Oh, Daehoon Hong, Sungho Jin and Frank E. Talke, IEEE International Magnetics Conference, May (2009)
5. “Planarization of Patterned Magnetic Recording Media for Improved Head Flyability”, Daehoon Hong, Chulmin Choi, Young Oh, Yeoungchin Yoon, Frank E. Talke and Sungho Jin, Magnetism and Magnetic Materials conference, November (2008)
6. “Effect of nanomagnet island diameter on switching field distribution in patterned media”, Chulmin Choi, Daehoon Hong, Mariana Loya, Li-Han Chen and Sungho Jin, 10th Joint MMM/Intermag Conference, January (2007)
7. “Switching behavior of nano patterned media with different side wall configurations”, Daehoon Hong, Chulmin Choi, Mariana Loya, Akihiro Inomata and Sungho Jin, 10th Joint MMM/Intermag Conference, January (2007)
8. “Intermediate layer Control in CoCrPt-SiO2 Perpendicular Media Recorded with Shielded Pole Head”, Hoonsang Oh, Hoosan Lee, Chulmin Choi, Younghoon Im, Youngsoo Kim, Noyeol Park, Magnetism and Magnetic Materials conference, November (2005)
9. "Thermal Stability of Magnetic Tunnel Junctions with New Amorphous ZrAl Alloy Films as the Under and Capping Layers", Chul-Min Choi, Jin-Oh Song and Seong-Rae Lee, IEEE International Magnetics Conference, April (2005)
10. “Thermal and electrical stability behavior of the magnetic tunnel junction with a new Zr-alloyed Al-oxide barrier”, Chul-Min Choi, Seong-Rae Lee, 9th Joint MMM / Intermag Conference, January (2004)
11. “Influence of insulating barrier thickness on the magnetoresistance properties of the magnetic tunnel junction with Zr-alloyed Al-oxide barrier” Chul-Min Choi and Seong-Rae Lee, 2003 International Symposium On Magnetic Materials and Application, December (2003)
12. “Surface roughness effects of bias voltage characteristics in magnetic tunnel junctions”, B. S. Chun, C. -M. Choi, I. C. Chu, S.-R. Lee, and Y. K. Kim, International Conference on Magnetism(ICM), July (2003)

ABSTRACT OF THE DISSERTATION

Nano Fabrication Approaches for Patterned Magnetic Recording Media

by

Chulmin Choi

Doctor of Philosophy in Materials Science and Engineering

University of California, San Diego, 2010

Professor Sungho Jin, Chair

Bit patterned media (BPM) have received increased attention in recent years as the primary candidate for 1 Terabit/in^2 or higher recording density. A patterned media consists of an array of well-defined magnetic nanostructures, each of which can store one bit of data. In the simplest scheme, the structures could be magnetic pillars and dots with a single easy axis of magnetization. The direction of magnetization is interpreted as a binary 1 or 0. Some of the main technical issues in the BPM include the difficulty in fabricating small nano-island arrays in a periodic fashion over large areas, reliability/reproducibility of magnetic bit characteristics, wear and head flyability issue which is associated with the media surface roughness, and processing cost. This thesis deals with investigation of various fabrication approaches, nanostructural features, and magnetic properties for the bit patterned media.

In Chapter 1, the science and technology of patterned magnetic recording media are discussed. In Chapter 2, fabrication of an array of high-coercivity magnetic Co/Pd multilayered islands using pre-patterned Si nanopillars template is described. The Si nanopillars have been prepared by advanced electron beam lithography (EBL) and reactive ion etching (RIE). In Chapter 3, the flying instability of the read/write recording head-slider on the topographically rough surfaces of the nano-patterned media is discussed, and technical approaches to overcome such a problem is described, such as planarization of nanopatterned topography by refilling the trenches and flatten the surface of the BPM. I have investigated the head flyability on BPM by fabricating nano pillar geometry with different topography. For flyability testing that requires a relatively large area, I have also fabricated nano pillars on 2.5 inch glass disks with a distribution of pillar size and periodicity using the "silver ball-up process" and RIE.

The process, structure and properties of planarized vs. non-planarized nano fabricated and imprinted BPM, are described in Chapter 4. A Si substrate was spin-coated with a thin PMMA layer, and a periodic island array was made by nano-imprinting lithography (NIL) with the patterned nanofeatures. The subsequent pattern transfer to the Si substrate was performed by using RIE process. A Co/Pd multilayer film was sputtered on the pre-patterned substrate. A HSQ layer was first spin coated on the patterned media to fill the trenches and subsequently re-etched by RIE to remove the overfilled regions on the substrate for planarization. In Chapter 5, the effect of magnetic island geometry on switching field distribution is discussed.

CHAPTER 1: Introduction

1.1 Background of the magnetic recording media

1.1.1 Superparamagnetism

Superparamagnetism is a phenomenon by which magnetic materials may exhibit a behavior similar to paramagnetism at temperatures below the Curie or the Neel temperature, but with higher magnetic susceptibility. Superparamagnets consist of single magnetic domains of elements that have ferromagnetic properties in bulk. Superparamagnetism is often associated with a small volume of ferromagnetic or ferrimagnetic nanoparticles as magnetization can randomly flip direction under the influence of ambient temperature. When the time of magnetic measurements is longer than the typical time between two suoerparamagnetic flips called the Néel relaxation time, the average magnetization appears to zero and the M-H magnetization loop displays zero coercivity and zero remanent magnetization at H=0.

Theoretical predictions concerning energetic stability of a single magnetic domain were established by Kittel in 1946 [1], defining a certain critical size of a particle. In smaller particles, the formation of a single ferromagnetic domain is often preferred. Moreover, it was shown by Neel, that at temperatures above the so-called blocking temperature T_B, a stable bulk magnetization cannot be established due to thermal fluctuations acting on small particles and consequently the system exhibits superparamagnetism [2]. At low temperatures (below T_B) the thermal fluctuations do not dominate and magnetic moments of superparamagnetism particles ’freeze’ in random orientation and cannot rotate freely.

The well known first model of magnetization reversal in a single-domain particle presented by Stoner and Wohlfarth [3] suggests an existence of high coercivity fields below T_B. At temperatures above T_B, the thermal effects allow flips of magnetic moments between the easy magnetization directions by getting over the energy barriers in zero field, and consequently the coercivity = 0. At temperatures ($T < T_B$) the thermal activation cannot overcome the magnetocrystalline anisotropy and the magnetic moment of each particle rotates from the field direction back to the nearest easy magnetization axis that yields a non-zero coercivity field. Since the nanoparticles and the corresponding easy magnetization directions are randomly oriented, the total magnetization is naturally reduced with increasing temperature.

Due to the enormous application potential of nanoparticles or nano-islands, the demand for these nanoparticles rises despite persistent difficulties in larger-scale fabrication. The high coercivity fields revealed for magnetic nanoparticle systems [4] make these materials interesting for applications in the area of high-density magnetic media.

The superparamagnetic effect in small, subdivided magnetic volume is a significant barrier to increasing magnetic data storage density in thin film magnetic data storage. The superparamagnetism is characterized by the ‘stability ratio’, defined in Equation (1) [5]:

$$\frac{K_u V}{k_B T} \qquad (1)$$

Where:

K_u is the uniaxial anisotropy energy density;

V is the switching volume;

k_B is Boltzman's constant;

T is temperature.

The top half of the equation is characteristic of the stored energy of the bit domain while the bottom half is the thermal energy of the domain. Clearly it is desirable to have this ratio as high as possible so that the thermal noise is negligible compared to the magnetic data energy. If the individual grain size (bit size) is continued to be reduced further to increase the areal density and storage capacity of hard disk drives, eventually the superparamagnetic effect will happen**.** In Figure 1, the coercitivity is plotted as a function of the size of the magnetic material for a single isolated particle. The domain structure of large magnetic particles tends to be subdivided by Bloch walls into magnetic domains. Therefore, the coercivity of a large magnetic particle tends to be less independent on the particle size. Further reducing the particle size leads to a size range (typically around ~20-200 nm regime), where the particles consist of only a single magnetic domain, which produces high coercivity due to the enhanced difficulty of magnetic switching in the absence of magnetic domain wall. Further decrease of the particle size eventually leads to a decrease of coercitivity to zero, when the thermal energy of the particle kT is larger than the energy of the magnetic anisotropy K_uV. This small volume phenomenon, called "superparamagnetism" is observed in many magnetic materials with relatively small magnetic anisotropy [6-8]

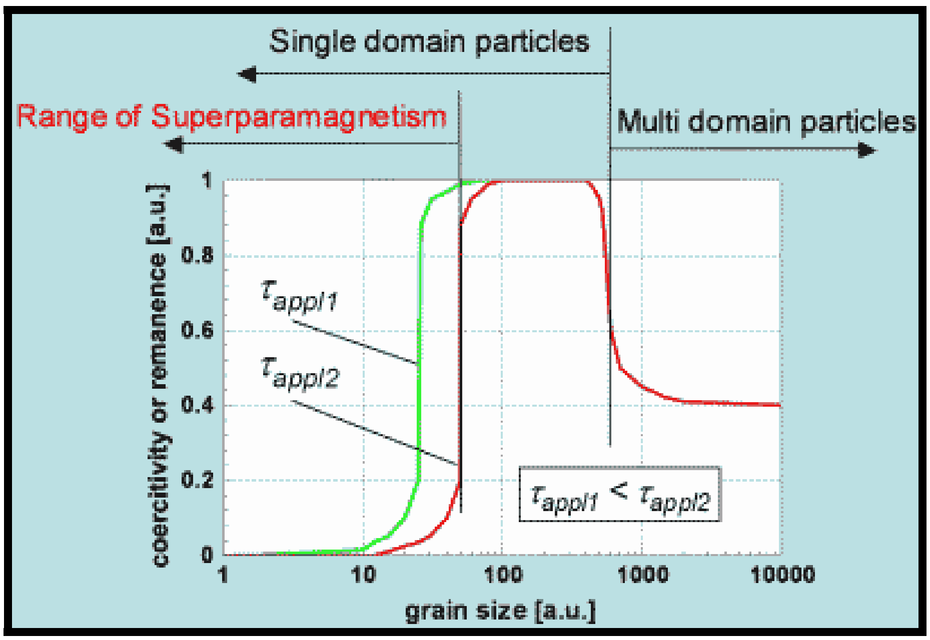

Figure 1. Coercivity as a function of grain size.

[http://www.nanoconsulting.de/englisch/mag_properties.html]

1.1.2 Conventional recording media

1.1.2.1 Longitudinal recording media

As indicated by the name, longitudinal recording is a method of recording data to a hard disk drive (HDD) in such a way that the data bits are aligned horizontally in relation to the spinning platter of hard disk drive, which is parallel to the surface of the disk. The longitudinal recording systems contain a recording head composed of a separate read and write element, which flies in close proximity to a granular magnetic recording medium, for example, the well known gamma iron oxide or Co-Cr-Pt alloy film with the random grains separated with thin walls of SiO_2. The inductive write element records the data in horizontal magnetization patterns. The information is then read back with the giant magnetoresistive read head by measuring the stray magnetic field from the transitions between regions of opposite magnetization. Finally a signal processing unit transforms the analog readback signal into a stream of data bits [9-11].

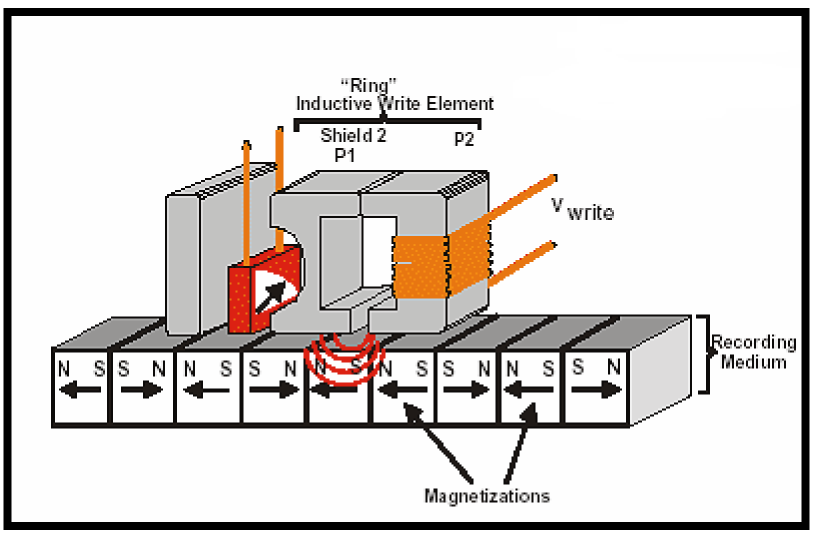

Figure 2. Schematic illustration of longitudinal recording technology.
[http://www.hitachigst.com/hdd/research/recording_head/pr]

1.1.2.2 Perpendicular recording media

In contrast, in thin film perpendicular recording media there is a SUL (soft magnetic underlayer, for example, made of a CoNbZr film) that guides the magnetic flux from the write pole to the collector pole which makes the easy axis of the recording media to be perpendicular to the film surface. Perpendicular recording differs from longitudinal recording in that data bits are aligned vertically (not horizontally), which allows for additional room on a disk to pack more data, thus, enabling higher magnetic recording densities. It is widely believed that with perpendicular recording [9-11], magnetic hard disk information storage density can be as high as ~700 gigabit/in^2 , however, this level of storage density is likely to be the upper limit. A new technology other than the simple perpendicular recording approach is required to advance the overall hard disk drive storage beyond the limit and reach a desirable density of 1 terabit/in^2 or higher.

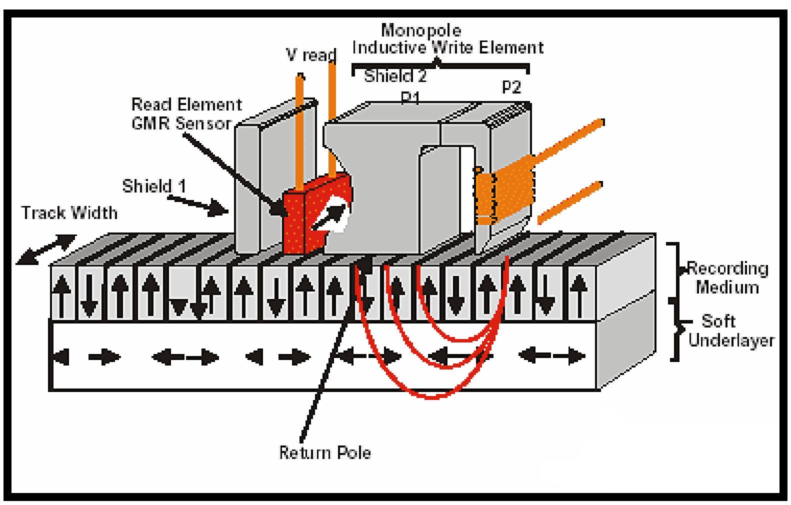

Figure 3. Perpendicular recording technology.

[http://www.hitachigst.com/hdd/research/recording_head/pr]

1.1.3 Patterned recording media

One of the most promising methods to circumvent the density limitations imposed by this "superparamagnetism" effect with smaller sized magnetic bits is the use of patterned media. In conventional media, the magnetic recording layer is a thin film of a magnetic alloy such as the Co-Cr-Pt alloy film with the random grains separated with thin walls of SiO_2. The recording layer naturally forms a random mosaic of nanometer-scale grains which behave as independent magnetic elements. Each recorded bit is made up of many of these random alloy grains.

However, in patterned recording media, the magnetic layer is created as an ordered array of highly uniform islands, with each island capable of storing an individual bit. This may be one grain, or several exchange coupled grains, rather than a collection of randomly decoupled grains. In the patterned media, single switching volume magnetic islands are formed along circular tracks with regular spacing. As the magnetic intrerference fluxes and associated emf voltage signals between adjacent magnetic domains in the granular alloy media can be essentially eliminated using physically separated patterned media islands, magnetic transitions no longer meander between random grains, but form perfectly distinct boundaries between precisely located islands. Since we no longer need on the order of ~100 grains per information storage bit for clean magnetic transition, the storage density in the patterned media with just one single switching volume can be increased in principle by about two orders magnitude compared to conventional recording media. Since each island is a single magnetic domain made of high vertical anisotropy material with high coercivity such as a $(CoPd)_n$ superlattice layer or FePt or CoPt type L1o phase alloy, patterned media is thermally more stable, even at densities far higher than can be achieved with conventional media.

The major advantages of such a scheme are --- first, the transition noise is eliminated because the bits are now defined by the physical location of the elements and not by the boundary between two oppositely magnetized (but physically in contact) regions of a thin film media. Second, very high data densities can be obtained because the stability criterion now refers to the volume and anisotropy of the entire magnetic element, not to the individual grains comprising the conventional granular media. Each of the magnetic switching elements could therefore become as small as a few nanometers [12-14], as compared to tens of nanometers.

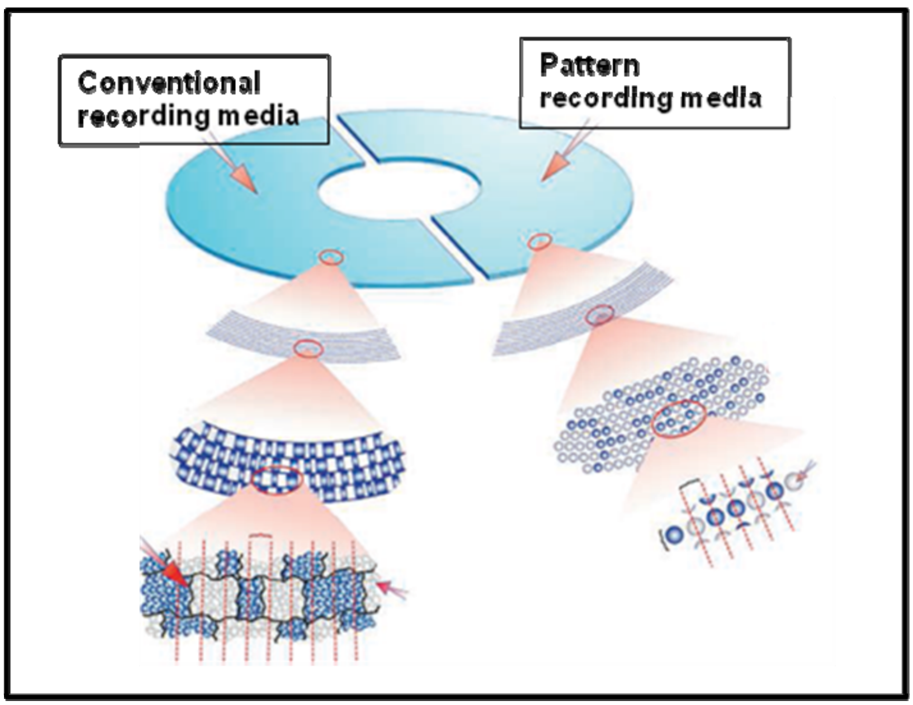

Figure 4. Conventional recording media vs. Pattern recording media.

1.2 Motivation of the patterned recording media research

1.2.1 Roadmap of hard disk drive (Areal density trends)

Figure 5 shows the recent trend of technology in the information storage industry. From 1998 to 2003, magnetic hard disk drive attained unprecedented growth in storage capacity, while the cost per gigabyte began to approach that of lower-cost magnetic tape. For example, during this period, magnetic hard disk drive prices dropped nearly 30 percent annually, while areal density increased at a rate of 100 percent per year. Yet, since 2003, hard disk drive manufacturers have been struggling with the physical limitations of current hard disk technology. Beginning in 2003, the increases in areal density began to slow down to about 34 percent per year. From figure 5, it seems apparent that the magnetic hard disk industry faces significant challenges to overcome the superparamagnetic and other physical limits to the continued increases in recording density required for higher computer disk capacities [15].

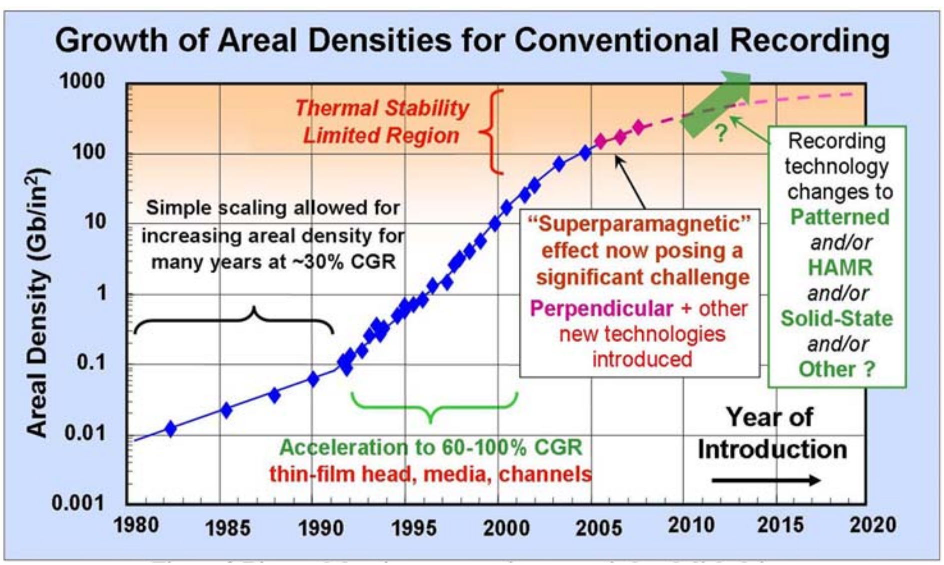

Figure 5. The trend of magnetic hard disk information storage technology.

1.2.2 Where are the needs for higher recording densities?

With modern computer technology and the enormous increase in the amount of information storage required, the whole world needs new, advanced technologies to store more data. While other competing technologies such as solid state memory (flash memory) and phase change memory are continually being improved, the magnetic hard disk technology still dominates because of superior stability/reliability of stored information together with ~two orders of magnitude lower cost per stored information bit. The required amount of information storage keeps increasing with additional consumer product related computer devices as well as the increased needs to store national security data and most likely individual medical and genome sequencing data in coming years. To ensure the best possible information storage density and higher quality in the data stored in computers, audio, video films, movies and games in consumer products including MP3 players, video recorders, video cameras, game consoles, netbook computers, iPhones and many other devices, a higher recording density media to store the information is essential. A higher recording density media also helps to miniaturize hard disk drive (HDD) for portable consumer electronic devices (e.g., netbooks and modern cell phones such as iPhones) without sacrificing the high-capacity requirement.

While there are clear needs for substantially increased information storage capacity, the lack of superior magnetic recording media has been the bottleneck for advances in modern storage technology. This research has been conducted in part to contribute to the advances in such a technology.

1.2.3 Approaches to avoid superparamagnetism problem

Superparamagnetism occurs when the size of each of the magnetically aligned particles in the recording media is so small that their magnetic energy is overcome by their own thermal energy. When this happens, they lose their magnetism quickly and become superparamagnetic with no coercivity and remanent magnetism. These particles are therefore unable to store information for any useful period of time, resulting in magnetic data instability, corruption and information loss.

Technologies intended to counter the effects of superparamagnetism and to increase the hard disk storage densities include the following:

- Thermally assisted recording: To achieve the desired level of information storage such as 1 Terabit/in^2, there is an evident conflict between the write magnetic field and the magnetic anisotropy (and coercivity) of the media. The magnetic anisotropy K_u must be increased by about one order of magnitude while maintaining a stability factor larger than 60 for reliable magnetic recording. K_u can be increased by one order of magnitude, for example, if one uses the FePt compound alloy based media (or other $L1_o$ phase based compounds such as CoPt) instead of the conventional perpendicular CoCrPt granular media with limited magnetic anisotropy. However, the required switching field of FePt (for polarity reversal on magnetic recording) can be as high as 50 kOe, which is very difficult to provide in practical sense. With the current technology, the magnetic field that the read/write head can provide never exceeds 17kOe. In order to overcome such a high coercivity problem in magnetic recording media, one approach is to utilize thermally assisted magnetic recording, which enables magnetic writing of high coercivity media. This method uses media with a very high K_u and writes data at high temperature where the coercivity is substantially reduced via laser beam or microwave beam heating of the local regions of the magnetic recording media that are about to be magnetically switched (data written). The written bits rapidly freeze during the cooling process, and the bits are stable at room temperature. [16-23] .

- Exchange-coupled composite (ECC) media: This media consists of magnetically isolated grains each consisting of two parts: a magnetically hard part with perpendicular anisotropy and a magnetically soft part where the anisotropy can point in any direction provided it is small. The lower-coercivity portion of the magnetic bit initiates (nucleates) magnetic switching at lower applied fields, with overall easier polarity switching of the magnetic bits. It can be quite promising anduseful for ultra high-density recording [24-29].
- Bit patterned media (BPM): This experimental technology replaces the currently utilzed media's continuous recording layer with a layer made up of microscopic, isolated magnetic regions created by lithographic, chemical or biological processes. These isolated regions support enhanced magnetic characteristics. In theory, this approach could yield data densities of more than one terabit per square inch. This technology is still evolving and many specific issues of fabrication, reliability and applications need to be resolved before large-scale industrial applications are realized. [30-32].

1.3 Fabrication of pattered recording media

Two major fabrication approaches have been employed for the bit patterned media (BPM). In the first approach, a layer of high coercivity magnetic material is thin film deposited on the flat substrate, e.g., using DC or RF sputtering. This layer is then directly patterned into discrete magnetic bits by using lithographic techniques such as ion beam milling, reactive ion etching (RIE), or focused ion beam milling (FIB).

In the second approach, the substrate is lithographically (E-beam, nano-imprint and block copolymer self-assembly) pre-patterned into islands before the magnetic material is deposited.

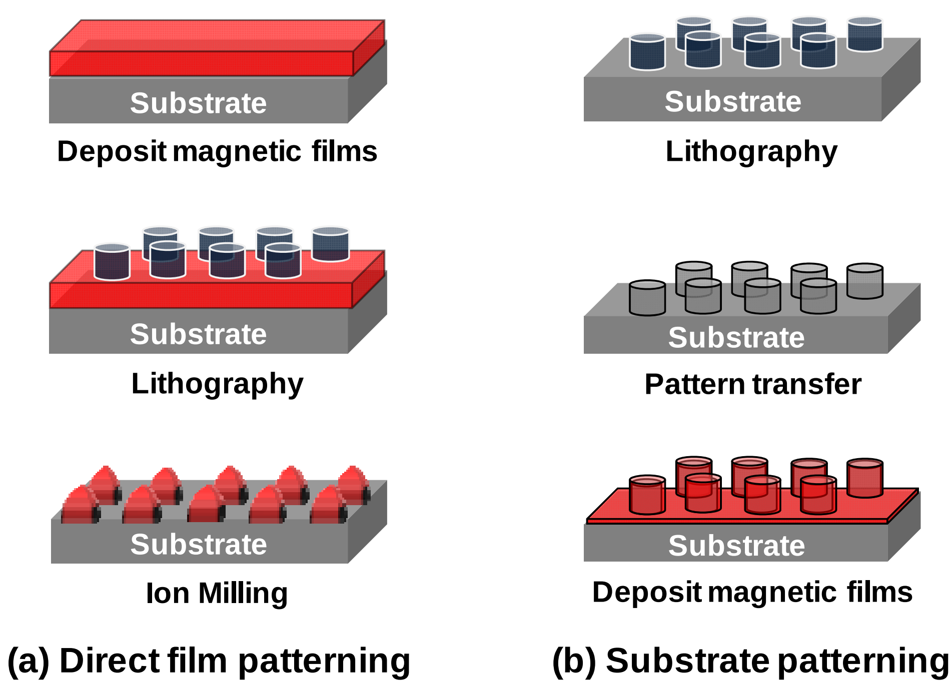

Figure 6. Fabrication of pattered recording media.

1.3.1 Electron-beam lithography

Electron-beam lithography is the most widely used patterning method for fabrication of nano scale patterns with dimensions of less than ~100 nm. For laboratory fabrication of patterned media with the magnetic island size in the range of 10 – 100 nm, the use of e-beam lithography is essential. Basically, the E-beam lithography consists of shooting a narrow, concentrated beam of electrons onto a resist-coated substrate. E-beam lithography can be generally divided into two methods of positive resist approach and negative resist approach (Figure 7). E-Beam lithography is also suitable for complex patterns like circles, rings, and for small structures. E-beam lithography technique is very similar with optical lithography which has been used for fabricating electronic devices. However, it uses electrons to draw a smaller pattern on the resist layer instead of UV light because the wavelength of electrons is much shorter than that of UV light. Thus, e-beam lithography leads to a higher resolution pattern. Resolution is not limited by diffraction limits, but by scattering of electron, the resolution is around 10 nm - 20 nm.

However, with such precision, components can only be made very slowly with a single e-bema source writing, and only one sample at a time, which greatly increases the time and cost, and prohibiting industrial manufacturing using the e-beam technology. Also, because electrons are charged particles, it is necessary to perform E-beam lithography inside a vacuum to avoid/minimize collisions with gas atoms present in the e-beam writer chamber environment, further complicating the required equipment and processes [33-35].

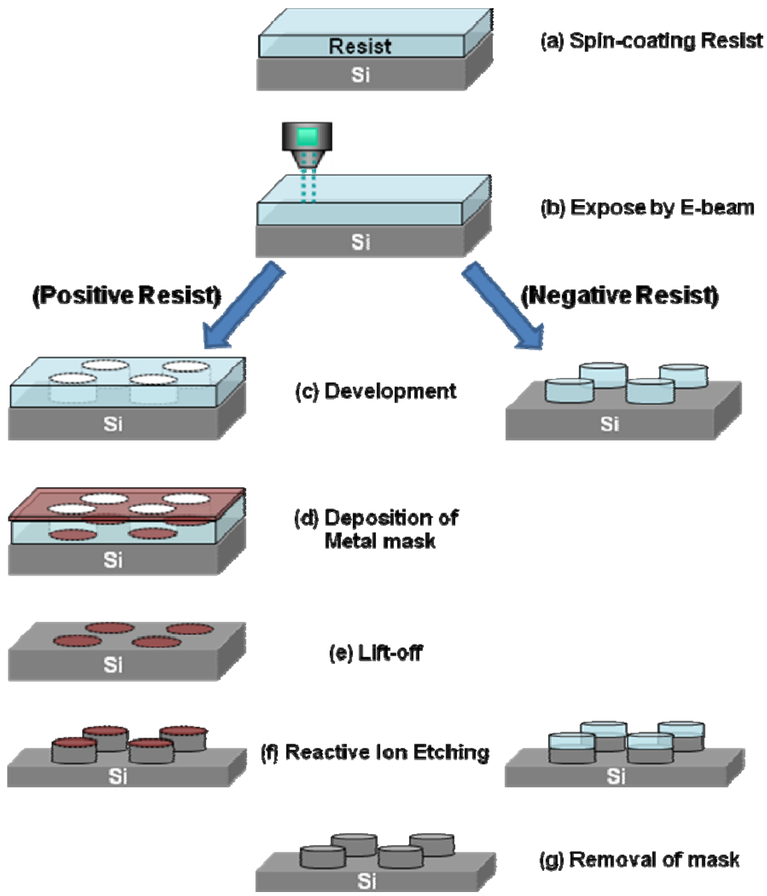

Figure 7. Fabrication using Electron-beam lithography

1.3.2 Nano-imprint lithography

Nano-imprint lithography can be utilized for high throughput nanomanufacturing of nano patterns and nano devices. There are two methods for Nano-imprint lithography (NIL). The difference between the two methods lies in the use mechanical compression vs UV light exposure using different types of polymer resist (thermorplastic polymer or UV curable polymer). A substrate is first coated with a thermoplastic or UV curable polymer layer, e.g., by spin coating. In the case of thermoplastic polymer, the polymer is heated to a temperature above its glass transition temperature and the stamp is pressed into the polymer. Thereafter, the polymer is cooled to below the glass transition temperature and the stamp and substrate are separated. In the case of UV curable polymer, ultraviolet light, passing through the glass imprint mask, is used to locally cross link the monomer and convert it to a polymer solid region. Because of this requirement the mold for the UV based nano-imprinting must be transparent. It is typically made of quartz. Thereby, the inverse profile of the stamp is replicated in the polymer. It can be transferred to the substrate using reactive ion etching [36]. Figure 8 shows this graphically.

Chou et al demonstrates an application of NIL to create patterned magnetic structures [37]. After pattern transfer to the substrate a metal is deposited into the NIL patterned holes by sputtering. The result is a rectangular pattern of dots of 10 nm diameter on a 40 nm period. With this technique, they fabricated nano-compact disk with 10 nm feature and 400 Gigabit/in^2 data density.

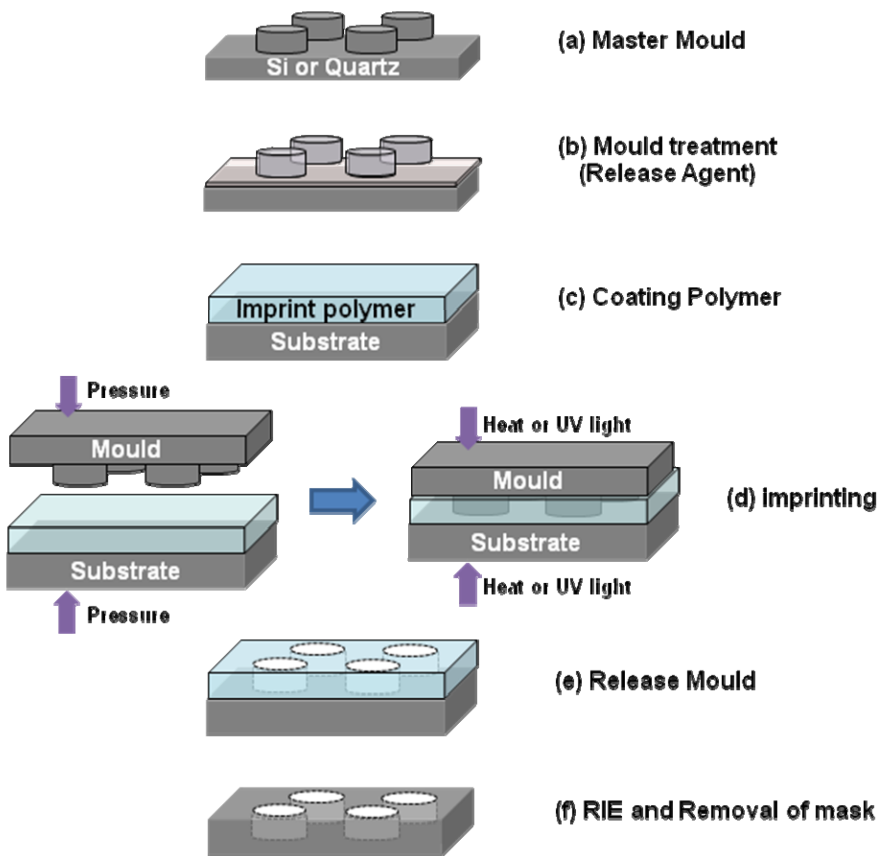

Figure 8. Fabrication of nano patterns using Nano-imprint lithography.

1.3.3 Block copolymer self-assembly

Diblock copolymers consist of two chemically different polymer chains (or blocks) joined by a covalent bond. Because of connectivity constraints and the incompatibility between the two polymer blocks, diblock copolymers spontaneously self-assemble into microphase-separated, nanometer-sized domains that exhibit ordered morphologies at equilibrium [38-39]. In a given diblock copolymer system, the relative chain lengths of the blocks determine the resulting morphology. Commonly observed microdomain morphologies in bulk samples are periodic arrangements of lamellae, cylinders, and spheres. The sizes and periods of these micro-domain structures are governed by the chain dimensions and are typically on the order of 10 nm. Structures smaller than 10 nm are also obtainable if one chooses appropriate blocks with a high Flory-Huggins interaction parameter [40] and decreases the block lengths. Diblock copolymer thin films spontaneously form nanometer-scale patterns over a large area, although long-range ordered structures such as needed for magnetic patterned media often require a special guided phase separation.

This diblock copolymer process is desirable for two reasons. First, the technique is relatively simple. It can be done in a standard chemical wet lab, with the addition of a spin coater and hot plate. Viewing the mask does require more expensive equipment, as standard facilities such as a scanning electron microscope (SEM), atomic force microscope (AFM) or similarly capable imaging device are often sufficient. Second, the diblock copolymer is desirable because of its low cost. Materials are relatively inexpensive and the process does not require expensive processing equipment. This combination makes thin film self assembly highly desirable.

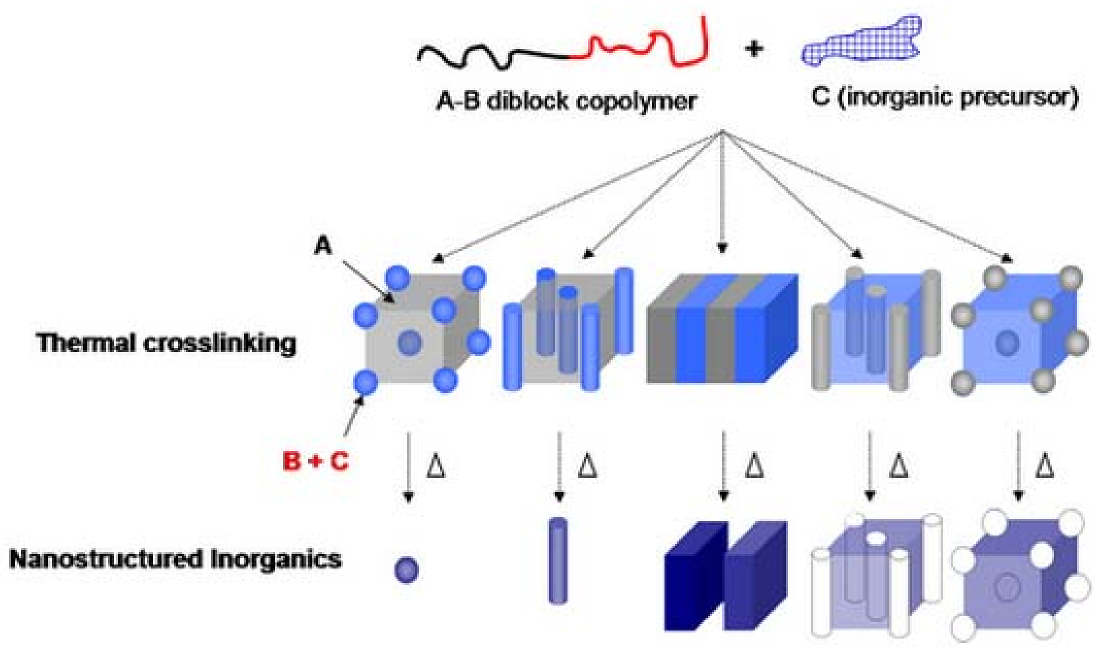

Figure 9. Schematic of block copolymer

1.3.4 Combination of E-beam lithography and block copolymer self-assembly

Self-organized macromolecular materials can provide an alternative pathway to conventional lithography for the fabrication of devices on the nanometer scale. In particular, the self-assembly of the micro domains of diblock copolymers within lithographically-defined templates to create patterns with long range order has attracted considerable attention, with the advantages of cost-effectiveness, large area coverage and compatibility with pre-established top-down patterning technologies. Block copolymers consist of two covalently bound polymer chains of chemically distinct polymer materials. The chains can self-assemble to form small-scale domains whose size and geometry depend on the molecular weights of the two types of polymer and their interaction.

Spherical morphology poly(styrene-b-dimethylsiloxane) (PS-PDMS) block copolymers, which have a large interaction parameter and a high etch-contrast between two blocks, can be templated using an array of nanoscale topographical elements that act as surrogates for the minority domains of the block copolymer [41]. Recently, complex nanoscale patterns can be generated by combining the self-assembly of block-copolymer thin films with minimal top-down templating. A sparse array of nanoscale HSQ (hydrogen silsesquioxane) posts were used to accurately dictate the assembly of a cylindrical PS-PDMS diblock copolymer into a wide assortment of complex, unsymmetrical features [42]. To extend the feature sizes to the sub-10 nm range, the formation of highly ordered grating patterns with a line width of 8 nm and period 17 nm from a self-assembled PS-PDMS diblock copolymer and sub-10-nm-wide tungsten nanowires were fabricated from the self-assembled patterns using a reactive ion etching process.

Beyond the rather limited morphologies of diblock copolymers, ABC triblock polymer thin films provide a diversity of new structures. For example, we obtained high-density nano-ring structures from a core-shell structured PS-PFSP2VP triblock terpolymer after the selective removal of PS and P2VP and square arrays of dots can also be achieved from a self-assembled PI-PS-PFS triblock terpolymer [39, 41, 43-50].

1.4 Thesis Outline

In bit patterned media, several challenges remain in making this technology practically useful for practical applications. Even though obtaining small dots (~10 nm in size) with a narrow spacing (~10 nm) by lithography is a challenge by itself. Also, planarization (a process by which the lithographically modified topography is flattened) is considered as another issue. If the disk is not planarized, the read and write head will have instability and drop in the flying heights.

In this thesis work, we have developed a practical fabrication technique to obtain good bit patterned media using e-beam lithography and nano-imprint lithography process. To control the deposited magnetic material placement, and to reduce the problem of the topological height of the bit pattern, we have investigated a simple and convenient planarization technique using spin coating of polymethyl methacrylate (PMMA) and hydrogen silsesquioxane (HSQ).

Chapter 1 gives a brief background on magnetic recording media including history, fabrications.

Chapter 2 discusses the fabrication of sub 10 nm Si patterned islands with sub 20 nm pitch.

Chapter 3 contains the head flyability on bit patterned media (BPM) by fabricating nano pillar geometry with different topography.

Chapter 4 demonstrates the process, structure and properties of planarized vs. non-planarized nano fabricated and nano-imprinted bit patterned media.

Chapter 5 describes the effect of magnetic island geometry on switching field distribution

Chapter 6 gives a summary of the main results in the work, discusses some of the ongoing research, and what needs to be done in the future.

The contents from the following papers have been included in the thesis:

1. Chulmin Choi, Yeoungching Yoon, Daehoon Hong, Young Oh, Frank E. Talke and Sungho Jin, “Planarization of Patterned Magnetic Recording Media to Enable Head Flyability”, (In preparation)
2. Chulmin Choi, Daehoon Hong, Young Oh, Leon Chen, Sy-Hwang Liou and Sungho Jin, “Enhanced Magnetic Properties of Bit Patterned Magnetic Recording Media by Trench-Filled Nanostructure”, (In preparation)

CHAPTER 2: The Fabrication of sub 10 nm Si Patterned Islands with sub 20 nm pitch

In this research, an array of Co/Pd multilayered magnetic islands on pre-patterned Si nanopillars template has been fabricated for construction of patterned media. The Si nanopillars have been prepared by electron beam lithography (EBL) and reactive ion etching (RIE). The diameter and pitch of the patterned pillars are sensitively affected by the properties of electron beam resist, developer chemistry combination and pattern transfer techniques. In this work, spin coated hydrogen silsesquioxane (HSQ) layer was used as the positive, high resolution e-beam resist. The smallest island size and pitch of the nano-patterned resist demonstrated was sub 10 nm and sub 20 nm with HSQ. We also used both a negative resist (Calixarene) and a positive resist (poly-methylmethacrylate (PMMA)) for comparison of nanofabrication processes and the resultant nano pattern quality. Co/Pd multilayer magnetic recording media films with a structure of Si\Ta 3nm\Pd 4nm\[Co 0.2nm\Pd 0.8nm]$_8$ were deposited on top of the patterned Si pillar array template by DC sputtering at room temperature

2.1 Introduction

The formation of high-density, nanoscale dot arrays is a challenging task. Such arrays are considered important not only for scientific study of the fundamental quantum-mechanical behavior of materials, but also for achieving a practical goal of ultrahigh-density data storage and manipulation devices [51-53]. In particular, methods for producing isolated high-density magnetic nanoscale arrays with a pitch of 25nm or less have been extensively studied with the aim of fabricating the next generation of patterned magnetic media with a recording density of 1 Terabit/in^2 and beyond [54-56]. With this application in mind, various fabrication attempts have been made, such as those based on a block copolymer, anodized aluminum oxide, colloid lithography, or laser interference lithography with extreme UV light [57-62]. However, electron beam lithography (EBL) based patterning technology still appears to be one of the most reliable routes for fabricating the patterned structures that are useful as molds for nano-imprint lithography (NIL) for eventual nanomanufacturing. The research by Hosaka et al., which demonstrated a calixarene resist dot array with a 25-nm pitch using a 30 keV accelerating voltage, appears to provide one of the best results reported to date [63]. While large areas can not readily be patterned with electron-beam lithography and it is still too slow for economic patterning, it can be used for the preparation of a limited number of masks for nano-imprint lithography (NIL) molds. Since the first proposal of NIL by Chou et al. in 1995 [64], many research groups have tried to fabricate NIL molds, in particular, for data storage applications [63, 65-66]. However, the progress toward fabricating NIL molds with high-density patterns and the subsequent pattern transfer by NIL has been somewhat slow during the last decade since the demonstration of a 400 Gigabit/inch^2 storage density in 1997 [65].

In this work, e-beam nano-patterning procedures using hydrogen silsesquioxane (HSQ) resists as well as PMMA and other resists, and the resultant nanostructures have been studied. The HSQ resist has some advantages over poly-methylmethacrylate (PMMA) and Calixarene because it is relatively robust against RIE plasma and ion bombardment. For research toward high density magnetic storage, an EBL process with thin HSQ resist using non-baking method and diluted buffered oxide etchant (BOE) development is being designed. The smallest island size and pitch of the nano-patterned resist that could be demonstrated was sub 10 nm with HSQ. Since the first use as an e-beam resist, HSQ has been demonstrated to exhibit fine resolution less than 10 nm on Si substrates with good shape transfer after development under optimized conditions.

2.2 Experimental details

2.2.1 Preparation of the Si nanopillar templates using PMMA (positive resist)

A typical EBL process for fabrication of the Si nano-template is schematically illustrated in Figure 10. The nano-templates were fabricated on (100) silicon wafers patterned with EBL and a reactive-ion-etch (RIE) process. PMMA A2 was two step spin-coated (500 rpm 5 sec, 4000 rpm, 40 sec) on the silicon wafers (See Figure 10a). Then it was exposed by electron beam to create a pattern of holes, which was performed by the Raith 50 E-beam writer located at UCSD Nano 3 Center (Figure 10b), with a beam radius of approximately 4 nm, an accelerating voltage 30 keV, and beam current 10 pA.. After exposure, the resist was developed (Figure 10c). A Cr metal layer (3 nm thick) was deposited on the whole surface of Si (Figure 10d). Only the Cr layer in the "holes" have direct contact with Si substrate and will remain on the surface after a lift-off process (Figure 10e). This patterned metal mask of 3 nm Cr was used to transfer this fine lithographic definition by RIE steps (Figure 10f). After RIE process, the Cr layer was etched with Cr etchant (Figure 10g). The morphology of the nanopillar arrays was visualized using a FEI field emission scanning electron microscope (SEM).

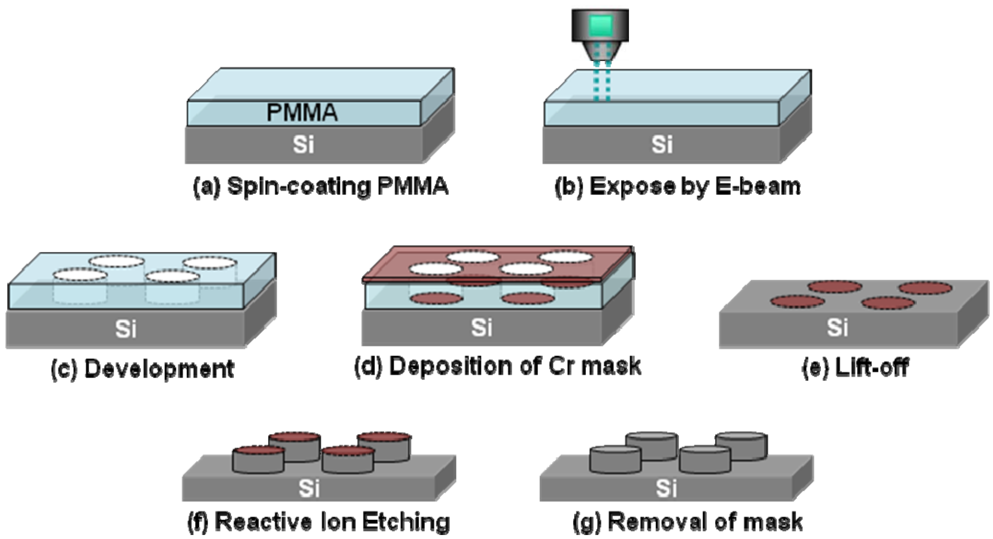

Figure 10. Schematic diagram for the EBL lithography process with a positive resist.

2.2.2 Preparation of the Si nanopillar templates using HSQ (negative resist)

Figure 11 schematically shows the procedures for EBL fabrication with HSQ and Calixarene. Diluted HSQ (Fox-12, Dow Corning) solution (Fox-12/methyl isobutyl ketone 1:2) was spin-coated on a Si substrate as a 40 nm thick layer and baked on a hotplate at 150°C. E-beam exposure was carried out with Vistec – VB300 equipment, with a beam radius of approximately 2 nm and an accelerating voltage of 50 - 100 keV. Dot-array patterns with various pitches ranging from 20 to 35 nm were exposed to an e-beam dose of 1.0–10.0 mC/cm^2. Resist development was carried out in a 2.5% Tetramethylammonium hydroxide (TMAH) aqueous solution at room temperature, followed by rinsing with diluted TMAH solution for 60 sec. In the case of sub 20 nm pitch, two sets of samples were prepared: one set was made by TMAH development process and the other set by TMAH solution and dilute hydrofluoric acid (HF) solution process. After resist development, dry etching was performed in a radiofrequency (RF) plasma chamber (Oxford Plasmalab 100). The Si substrate with patterned HSQ was then etched in a gas mixture of C_4F_8 and SF_6 using RIE (Oxford Plasmalab-100) for pattern transfer into the substrate. After the dry-etching step, the residual HSQ was removed.

2.2.3 Preparation of the Si nanopillar templates using Calixarene (negative resist)

The procedure for the Calixarene negative resist is similar to the HSQ process. The Calixarene resist(Yamamoto chemicals, Japan) was spin-coated (3000 rpm, 30 sec) on a Si substrate as a 30 nm thick layer after hexamethyldisilazane (HMDS) treatment and then prebaked in air on a hot plate at 110°C for 60 s. After that, the e-beam exposure was carried out using the Raith 50 E-beam writer. After exposure, samples were developed using isopropyl alcohol (IPA) at room temperature for 60 sec.

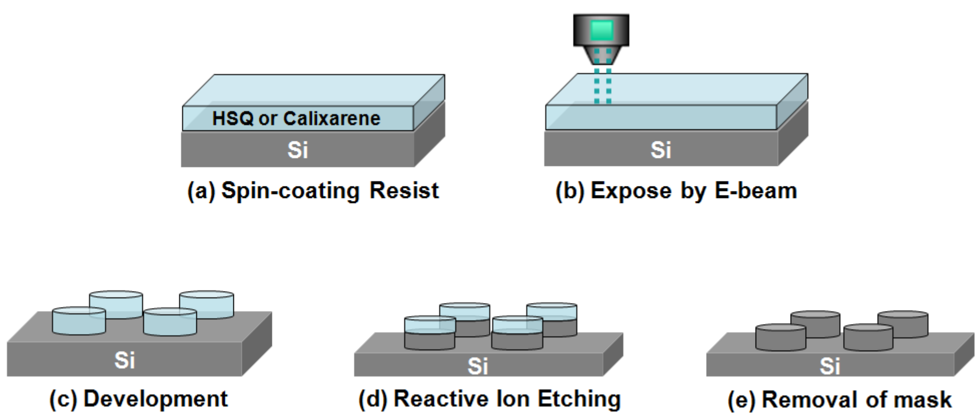

Figure 11. Schematic diagrams of EBL lithography process with negative resist.

2.2.4 Magnetic thin film deposition

$(Co/Pd)_n$ multilayer magnetic recording media film with a perpendicular anisotropy [Ta 3nm\Pd 3nm\[Co 0.3nm\Pd 0.8nm]$_8$] structure was deposited on the top surface of the patterned Si template by a four-target DC magnetron sputtering system at room temperature, under a typical base pressure below ~5×10^{-7} Torr.

2.3 Results and Discussion

2.3.1 Si nanopillar templates using PMMA

PMMA is the most frequently used electron beam resist with sub 30 nm resolution. PMMA needs a low e-beam exposure dose writing because it exhibits a high sensitivity to electron beam. To prepare highly-packed patterns using PMMA with a thickness of about 30 nm, the exposure dose used was relatively low (300 – 500 $\mu C/cm^2$) and the exposed sample was developed using a new developer (IPA:DI Water) with cold ultrasonic development [67]. Figure 12 shows SEM images of Si nanoscale pillar arrays after etch mask deposition, lift-off, and RIE processing. The image in Figure 12a shows nano pillars with conventional development process using IPA:MIBK solution. The protruding Si islands have a dimension of ~40 nm diameter and ~100 nm pitch. On the other hand, the Si pillar arrays produced with a new developer (IPA:DI Water) exhibit a much better resolution (e.g., 30 nm diameter and 50 nm pitch) with cleaner nano island geometry (Figure 12b). The resolution can be improved by adjusting different steps of the lithographic development process.

Co/Pd multilayer magnetic recording media film with [Ta 3nm\Pd 3nm\[Co 0.3nm\Pd 0.8nm]$_8$] structure were deposited on top of the patterned Si template with 40 nm diameter by DC magnetron sputtering system at room temperature (Figure 13). The magnetic properties of the continuous and patterned Co/Pd multilayer films were measured by alternating gradient magnetometer (AGM) and magnetic force microscope (MFM). As shown in Figure 14a, unpatterned Co/Pd multilayer has square loop with high perpendicular anisotropy. However, the area of patterned Co/Pd multilayer (1 μm × 1 μm) contained too little magnetic materials volume for M-H loop and coercivity measurements using SQUID magnetometer. To measure the magnetic property of this small area, the micro magneto-optical Kerr effect (micro-MOKE) apparatus at Hitachi GST was utilized. We also measured the MFM image of a patterned Co/Pd multilayer after DC erasure by using a 3,000 Oe magnetic field. Figure 14b shows that most of the dots have perpendicular magnetization. The black spots and white spots mean magnetization reversal (spin up and spin down). Despite the use of a 3,000 Oe applied magnetic field, the dots do not have one magnetization direction (saturation). In general, patterned media with smaller nano-islands exhibit higher magnetic switching field, and a higher coercivity is anticipated for the island configuration in MFM measurements such as shown in Figure 14b.

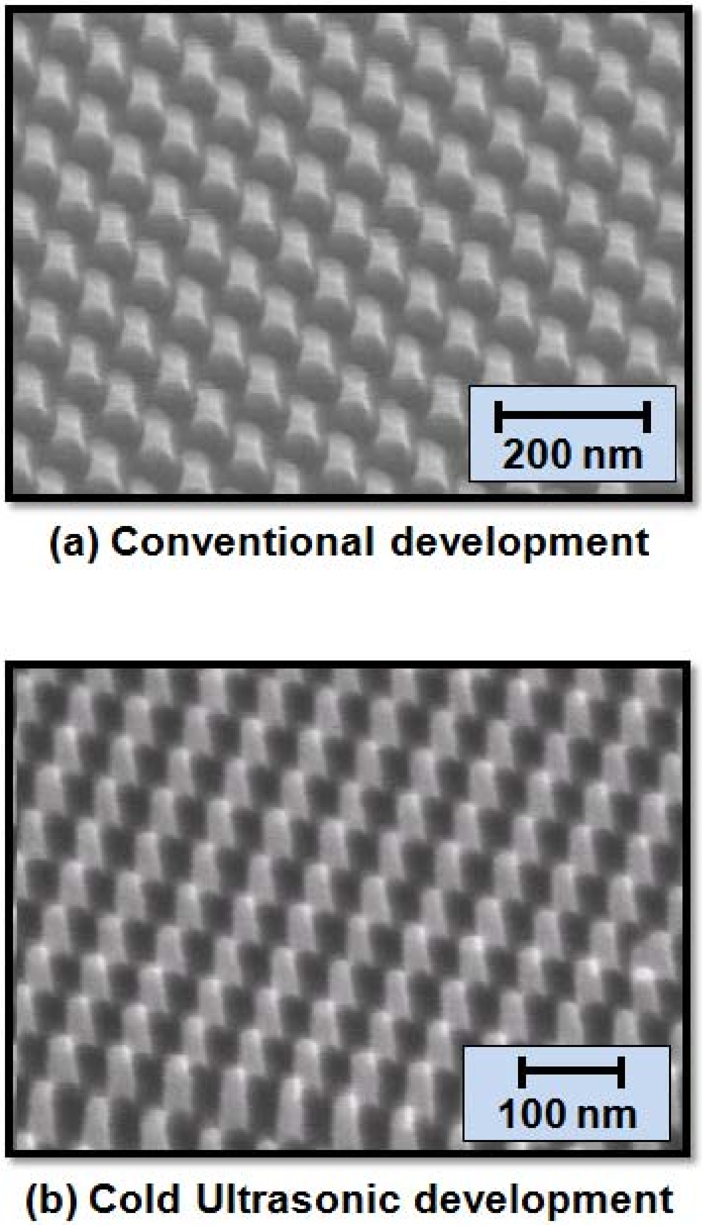

Figure 12. SEM images of Si nanoscale pillar arrays with (a) conventional resist development and (b) cold ultrasonic development.

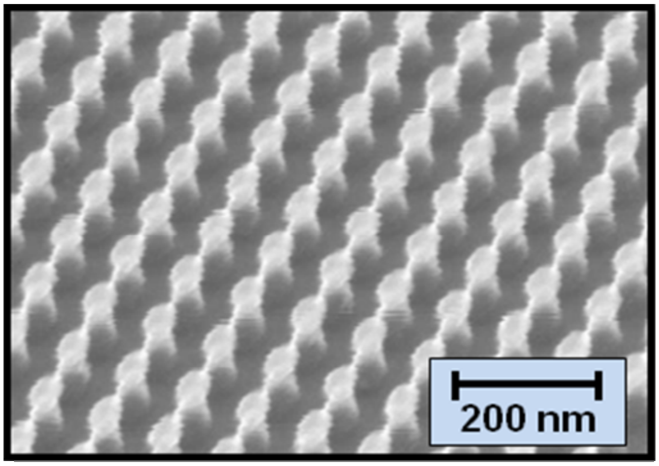

Figure 13. SEM images of after Co/Pd multilayers deposition on Si template with 40 nm diameter.

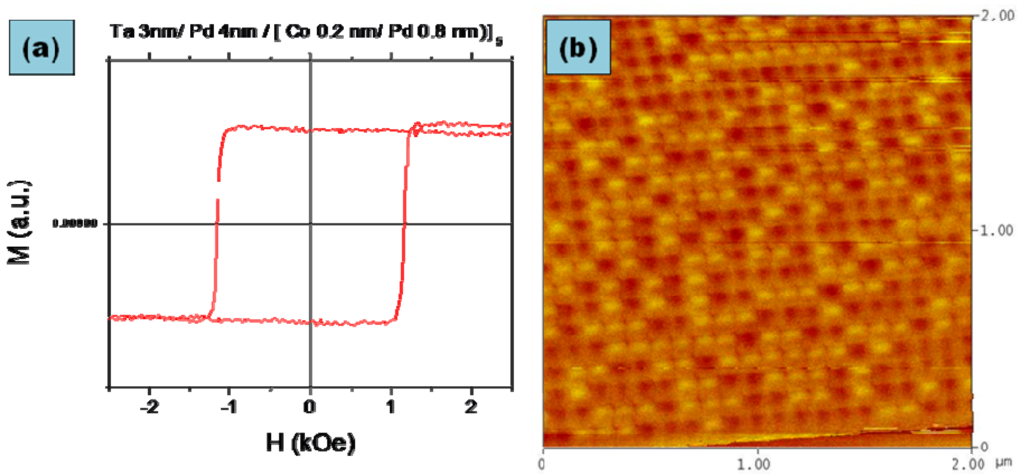

Figure 14. (a) Magnetic hysteresis loops for unpatterned Co/Pd multilayer. (b) MFM image for patterned Co/Pd multilayer.

2.3.2 Si nanopillar templates using HSQ

Figure 15 shows SEM images of HSQ nanodot arrays after the development step for various pattern pitch sizes. HSQ nanodot arrays with pitches ranging from 35 to 20nm were successfully fabricated. The HSQ resist has a high resistance against the dry etch process. Figure 16 is the Si nanopillar arrays after the overall pattern transfer process (EBL lithography and RIE) with a variation in the pattern pitches of a) 35, b) 30, c) 25, and d) 20 nm. The 10 nm island array (20 nm Si pitch island array), Fig. 16(d), corresponding to a quite high areal density of 1.6 Terabit/inch^2 was successfully fabricated. Higher density dot arrays beyond the the 1.6 Terabit/inch^2 (20 nm pitch) was not successful due to the formation of many defects. It needs further improvements in EBL procedures.

Figures 16 is an SEM image of a Si pattern with various pitch sizes after Si etching by the RIE system using HSQ as a hard mask and new develop method. This new develop method will be discussed in more detail later. As shown in Figure 17a, transfer of the resist pattern with 20 nm pitch to the Si substrate using conventional develop method was unsuccessful. This is believed to be due to the insufficient isolation of each dot in the resist pattern after the development step. As a result, the resist patterns became blurred and finally disappeared during the plasma-etching step. The residual resist between the neighboring dot patterns after the development step (often referred to as a resist scum) can be seen from Figure 17a. The resist scum is caused primarily by the e-beam proximity effect from the scattering of incident electrons in the resist and substrate [68-69], although other effects such as unintended polymer crosslinking in the regions between the dots may also contribute. To remove residual resist material between the dot patterns and get the well isolated HSQ dot pattern, a dilute HF solution instead of conventional method with only TMAH solution was used. During the development process of HSQ resist in a TMAH solution, HSQ surface tends to have the formation of a TMAH insoluble siloxane layer. Using the modified process, the resist scum could be eliminated and a sub-20 nm pitch island array with ~10 nm diameter, which corresponds to a high areal density of 1.6 Terabit/inch^2 Si nanopillars, was successfully obtained (Figure 17b).

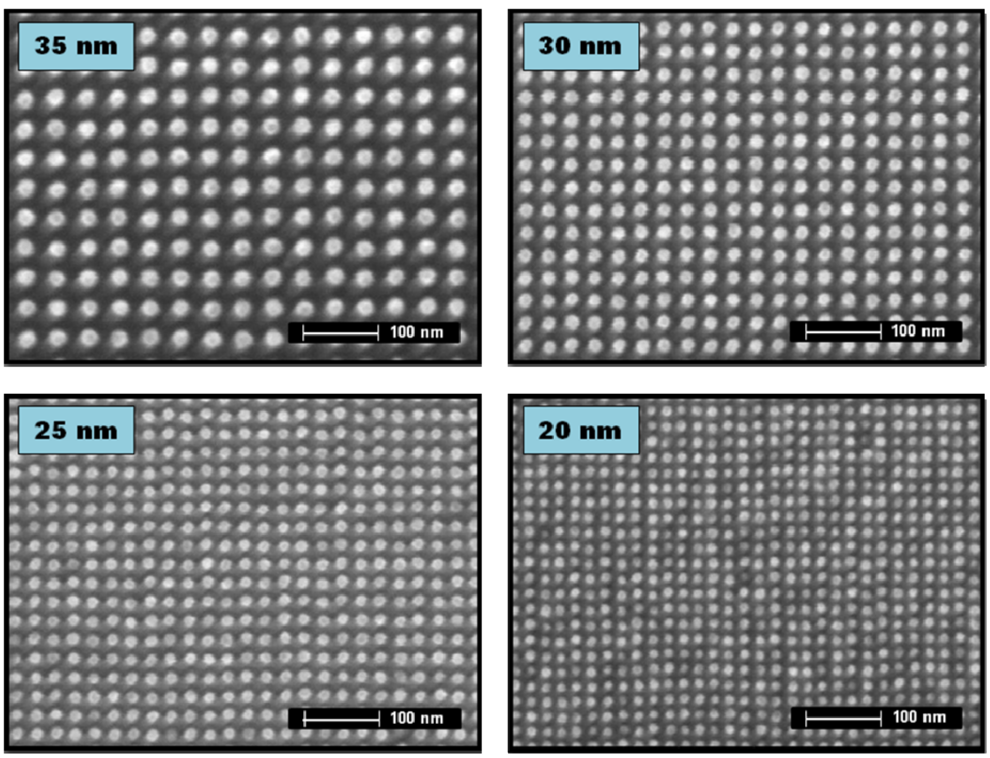

Figure 15. SEM images of HSQ resist nanodot arrays after the development step for various pattern pitch sizes.

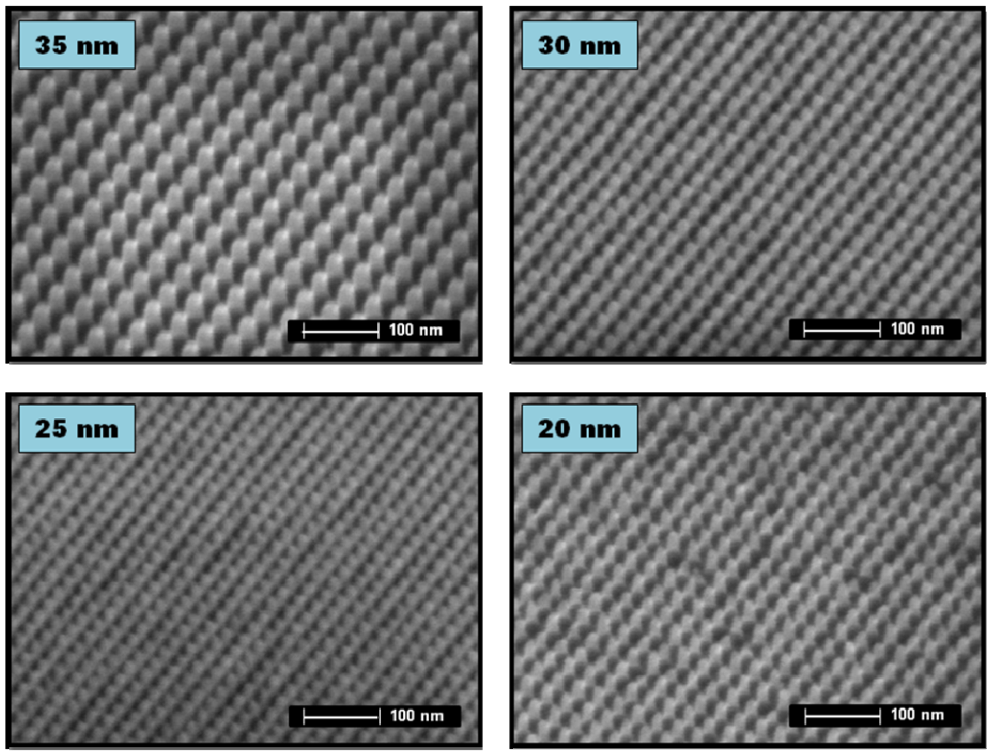

Figure 16. SEM images of the Si nanopillar arrays after the overall process (EBL lithography and RIE) with a variation in the pattern pitches of a) 35, b) 30, c) 25, and d) 20 nm.

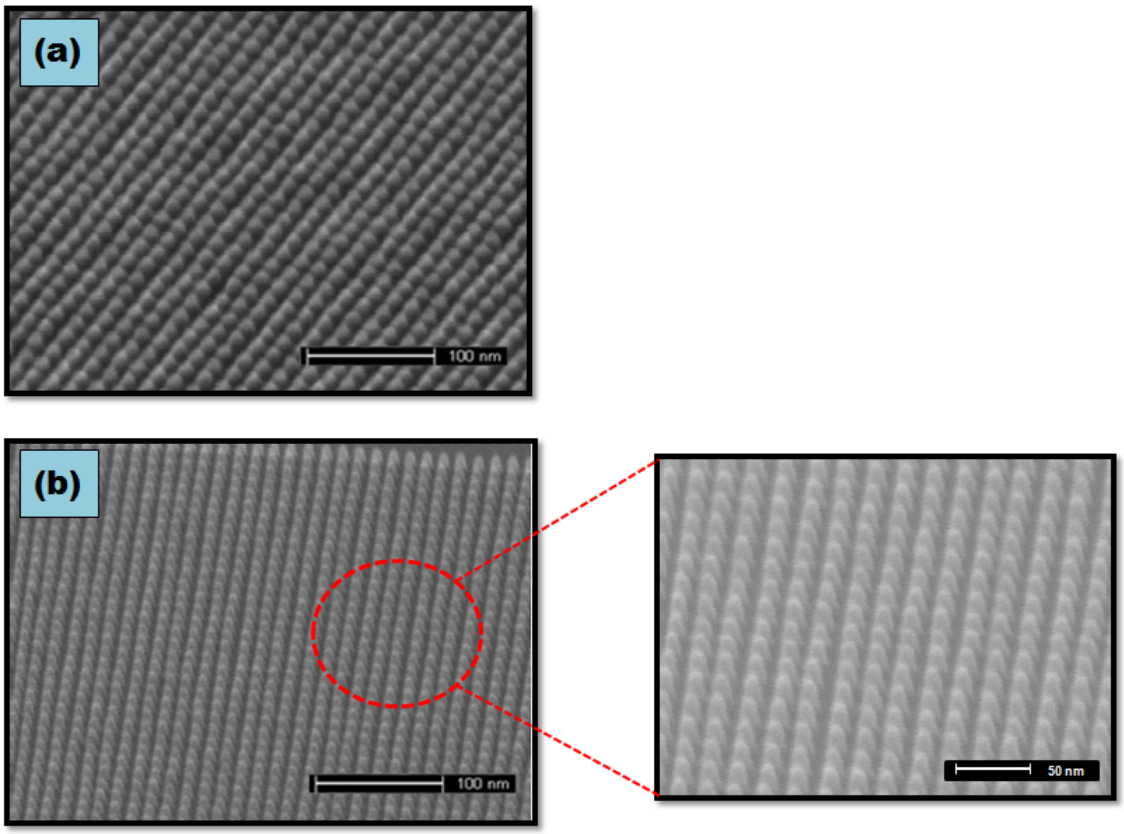

Figure 17. SEM image of a Si pattern with 20 nm pitch after Si etching by the RIE system using HSQ as a hard mask.

2.3.3 Si nanopillar templates using Calixarene

Figure 18 shows an SEM image of typical dot patterns obtained using the Calixarene resist on a Si substrate. The diameter of the dots and the pitch of the dots are 15 nm and 30 nm, respectively. This dot pattern is almost the same as for HSQ. However, transfer of the resist pattern to the Si substrate was unsuccessful and somewhat smeared pattern was observed because the Calixarene resist is not strong enough to withstand the RIE process.

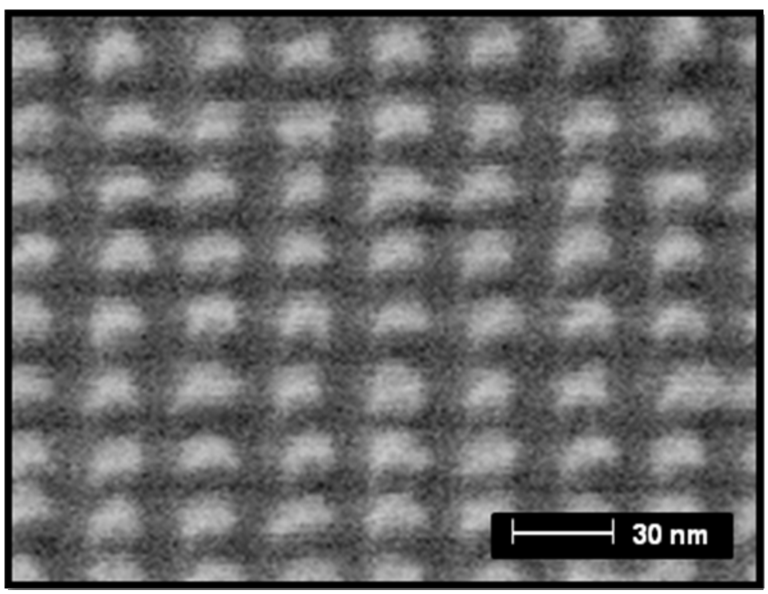

Figure 18. SEM image of typical dot patterns of the Calixarene resist on a Si substrate.

2.4 Summary

One positive and two negative EBL resists, PMMA, HSQ, and Calixarene were patterned by 30 - 100 kV E-beam lithography process and a subsequent pattern transfer into silicon has been characterized and compared. A highly anisotropic RIE process was developed to transfer the written patterns into silicon. It is expected that these process improvements will be useful for developing practical fabrication techniques for bit-patterned magnetic media.

CHAPTER 3: Planarization of Patterned Magnetic Recording Media to Enable Head Flyability

Bit patterned media with topographical surface roughness do not allow the read/write head slider to fly for magnetic information storage and retrieval. Here the planarization of the patterned magnetic recording media was investigated in order to enable head flyability. Various nano pillar geometries with different topography were investigated. Firstly, nano pillars arrays with 40 nm diameter and 60 nm height were fabricated by e-beam lithography and reactive ion etching (RIE) to demonstrate the planarization process for patterned media. Since the read/write head flyability test requires a much larger sample area in a disk configuration, we have prepared a similarly topographically rough surface on a 65 mm dia. (2.5 inch) glass disk by using a "silver(Ag) ball-up process" and reactive ion etch (RIE). To obtain the large area samples, we also fabricated nano pillars on 65 mm (2.5 inch) glass disks with magnetic bit islands having a distribution of pillar size and periodicity. The magnetic island bits consisting of a multilayer of Ta 3nm\Pd 3nm\[Co 0.3nm\Pd 0.8nm]$_8$ were sputter deposited on the top of the nano pillars and planarized with hydrogen silsesquioxane (HSQ) by spin coating. The HSQ layer was back-etched using RIE, resulting in a smooth surface. The planarization process was found to allow recording head flying on the recording media surface. The new planarization technique is easier to process and more reliable than the conventional planarization with SiO_2 and subsequent chemical mechanical polishing (CMP).

“Flyability testing” indicates significantly improved flying stability of typical magnetic recording sliders on the topographically rough disks, with the standard deviation of flying height fluctuations being only on the order of 0.1 nm. The latter value is essentially comparable to that of unpatterned smooth disks.

3.1 Introduction

Hard disk magnetic recording is one of the crucial information storage technologies for computer operations. Bit patterned recording media (BPM) have received increased attention as the primary magnetic information storage candidate for 1 Terabit/in^2 or higher recording density [55, 70]. As the magnetic bit size in conventional granular media is reduced for higher recording density, the magnetic energy becomes too small to prevent thermally activated bit reversal. For BPM, the switching volume is identical to that of an individual bit since the bits are lithographically pre-defined. The bit is desirably as small as 10 nm or less, and should be thermally stable against undesirable switching. The BPM is expected to have a sharp magnetic transition and low noise because the transitions, both along and cross a track, are now defined by the patterned bits, as compared to the head fields and grains with size distributions in the media.

It is well known that two major fabrication methods exist for BPM [71-73]. In one method, a layer of high coercivity magnetic materials is first deposited on the flat substrate. This layer is then directly patterned into discrete magnetic bits by using lithographic techniques such as ion beam milling, reactive ion etching (RIE), or focused ion beam milling (FIB). The main advantage of this method is that no magnetic material is left between neighboring bits to cause any interfering magnetic signals. In addition, roughness on the media surface can be small because the height of the bits can be as small as the thickness of the recording layer. However, a main disadvantage of this method is that the magnetic material can easily be damaged by the ion etching patterning process. Furthermore, the metallic magnetic material removed during the ion-etching process can be re-deposited on the media during the patterning process, which is undesirable. In the second method, the substrate is lithographically pre-patterned into protruding islands before the magnetic material is deposited. The main advantage of the latter method is that the magnetic material deposited on the top of the pillars is isolated from adjacent islands without the need for ion milling or other etching methods, and, thus, there is no damage of the magnetic material. However, the magnetic material in the trenches can introduce undesirable noise during the read/write process and can cause magnetic interactions between the magnetic materials deposited in the trench and on the top of the islands.

In order to minimize magnetic interactions of this latter type, the height of the bit pattern, i.e., the height of the individual pillars, should be “large” enough so that the trench magnetic material contributes minimally to the signals picked up by the flying read/write head. However, protruding pillars of large height exert a significant influence on the flying characteristics of magnetic heads than pillars of small height because of physical and aerodynamic interference by the surface topography on moving head which is typically designed to fly with only several nanometers spacing from the magnetic media. In fact we have observed that the bit patterned media does not even allow flying of the read/write head if the nano trench depth is ~40 nm or deeper. The loss of flying height of a slider on bit patterned media is anticipated to be more severe with the height (depth) of the bit pattern. To reduce such a topography effect of the bit pattern (pillar height), it is necessary to fill the trench space with a nonmagnetic material to create a “smooth” disk. The process of filling the trench regions around protruding bits is called “planarization”. It has been reported by Hattori et al. [74] that a deposition of SiO_2 by sputtering and removal of the excess SiO_2 by chemical mechanical polishing (CMP) is an effective method for planarization of BPM. However, the CMP process is generally delicate and time-consuming, and a damage of magnetic material could occur during the mechanical/chemical polishing process.

In this work we demonstrate a simple and efficient planarization method for the BPM type surface containing nanoscale protruding topography. We use hydrogen silsesquioxane (HSQ), a commonly used negative resist, to fill and planarize the nano-topographically patterned recording media, which on annealing converts to mostly silicon oxide material. The HSQ can easily be spin-coated to fill the etched trench areas. In addition, the mechanical properties and thickness of hydrogen silsesquioxane (HSQ) can be controlled for optimum flyability by altering and/or controlling the post-deposition baking temperature and plasma treatment. After spin-coating, HSQ is back-etched by RIE (reactive ion etch) to remove most of the excess material beyond the top surface of the magnetic bits. Flyability tests with the planarized BPM were performed, which demonstrated excellent flying characteristics.

3.2 Experimental details

Figure 19 schematically illustrates the processes for BPM fabrication and subsequent planarization employed in this research. A Si wafer was spin-coated with a 40 nm thick layer of HSQ (hydrogen silsesquioxane resist, Dow Corning No. Fox-12). The local areas to be patterned were exposed by an electron beam, followed by a resist development process using tetramethylammonium hydroxide (TMAH). The Si substrate with patterned HSQ was then etched in a gas mixture of C_4F_8 and SF_6 using RIE (Oxford Plasmalab-100) for pattern transfer into the substrate (Figure 19(a)).

In order to produce the nano-topography pattern on a large area required for flyability tests, we prepared a protruding nano-pattern on a 65 mm (2.5 inch) glass disk substrate. Although the nano-pattern on this larger-area sample does not have a periodic array pattern, it has nevertheless the nano-topography pattern with desired level of surface roughness on the whole glass disk substrate. To simulate the nano topographic roughness and test the read/write head flyability on the whole disk, a thin film sputter deposition of Ag film was conducted, followed by subsequent annealing in vacuum at temperatures of up to 650 °C to break up the film into islands. In this paper we denote this process as “ball-up process” because of the spheriodization type change of film morphology casused by break-up of continuous film. The “balled-up” Ag nano islands were then used as an arrayed nanoscale etch mask to subsequently pattern transfer onto the underlying glass disk surface using the same RIE process as described above.

A magnetically hard Co/Pd multilayer film with a {Ta 3nm\Pd 3nm\[Co 0.3nm\Pd 0.8nm]$_8$} structure having desirable perpendicular magnetic anisotropy was sputtered on the pre-patterned substrate (Figure 19(b)). The coercive force of the Co/Pd multilayer was in the region of ~3,000 Oe, an appropriate value for magnetic recording. A HSQ film was first spun on the patterned media to fill the “trenches” (Figure 19(c)) and subsequently re-etched by RIE to remove the “overfilled” regions on the disk. The disk was then baked on a hotplate at 110 °C for 180 sec to vaporize the solvent in HSQ (Figure 19(d)). The HSQ was mechanically hardened by oxygen plasma irradiation using RF RIE (Figure 19(e)). The gas flow rate, pressure, and RF power used for the RIE process were 50 sccm, 100 mTorr, and 300 W, respectively. For flyability testing, a diamond like carbon (DLC) film of 5 nm was sputtered on the planarized BPM media and a thin lubricant (Zdol 2000) was applied by dip coating similarly as for hard disk drive operations. The surface roughness of the planarized BPM media was analyzed by atomic force microscopy (AFM) and scanning electron microscopy (SEM). The head flyability was evaluated before vs. after planarization.

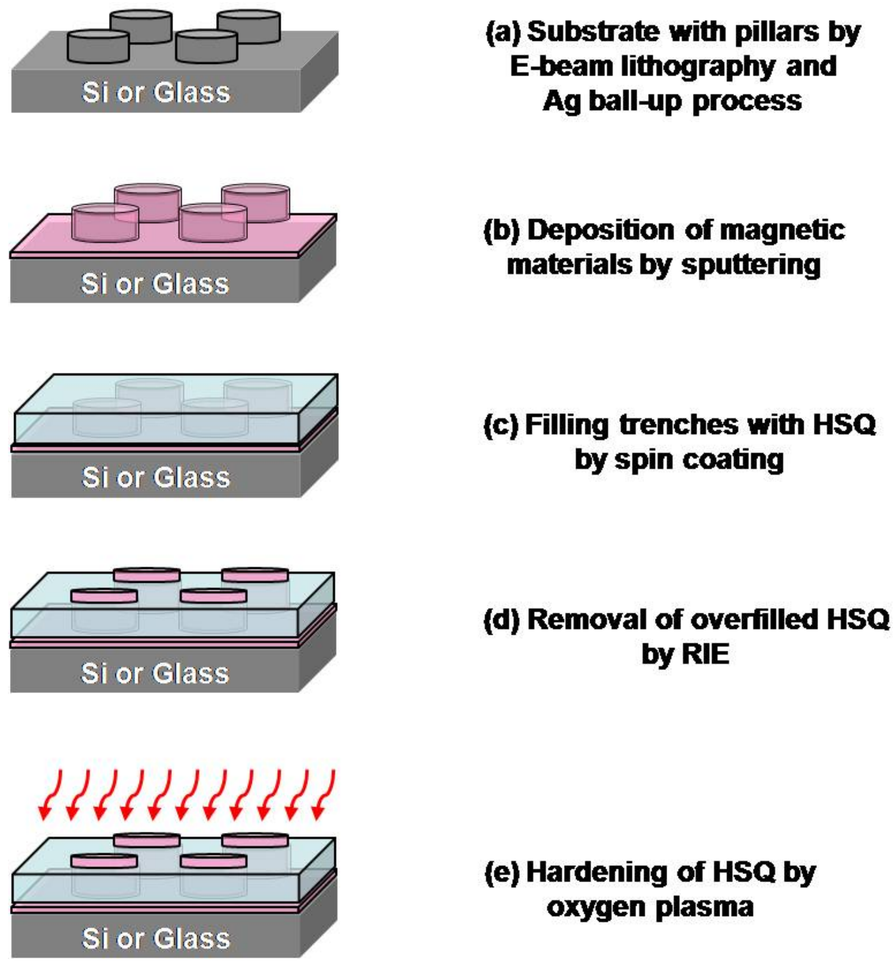

Figure 19. Schematic diagrams of the fabrication process for bit patterned media (BPM).

3.3 Results and Discussion

The "nano pillar" pattern was fabricated using two different lithography techniques. Nano pillars with periodicity and an island diameter of ~40 nm were created by using a negative e-beam resist (HSQ) and e-beam lithography. Shown in Figure 20(a) is an oblique angle SEM picture of an example bit patterned media that we fabricated by e-beam lithography, with the protruding Si islands having dimensions of ~40 nm diameter and ~60 nm height, with an equivalent memory bit density of ~0.15 Terabit/in^2. A higher-density pattern with 10 nm diameter bit array (1.6 Terabit/in^2 density) was also fabricated as shown in Figure 20(b).

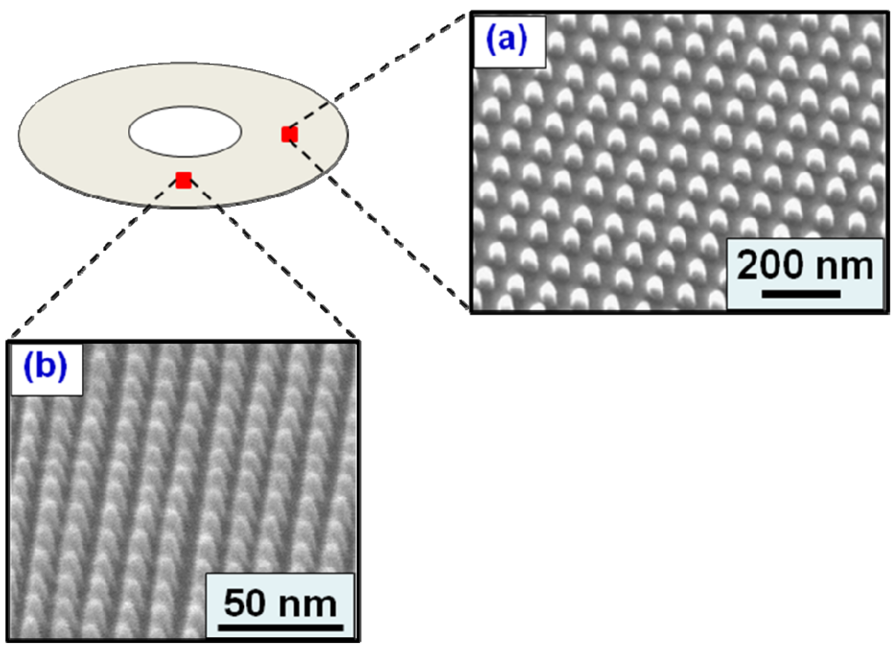

Figure 20. (a) Oblique angle SEM images showing topographical features of bit patterned media (30 nm diameter bit array (~0.18 Terabit/in^2 density)). (b) 10 nm diameter bit array (1.6 Terabit/in^2 density).

With such a three-dimensional topography, magnetic read/write head at a few nanometer operational spacing off the media cannot fly because of surface roughness and aerodynamic interferences.

In order to optimize the planarization condition and test head slider flyability of the fabricated bit patterned media (BPM), a 65 mm (2.5 inch) disk sized large area is required. However, R&D toward manufacturing of such a large area with uniform nano-islands is still in progress, and it would be costly and time consuming in the laboratory to fabricate such a large disk with precise nano-patterning for flyability testing. As an alternative, we created nano-topography with a distribution of nano-islands and used this type of disk media to understand flyability aspects of nanoscale protruding surface structures. To produce a distribution of magnetic nano-islands, without using expensive e-beam lithography, we used a metal island mask produced via the “ball-up” process described above. The SEM image of typical nano pillars obtained in this way is shown in Figure 21(a). The height of the pillars created on the glass substrate is ~40 nm. This height is considered to be large enough to avoid magnetic interactions of the recording media material deposited in the valleys with that on the top of the pillars. Since the patterned surface leads to slider instability, the media surface needs to be planarized. The image in Figure 21(b) shows nano pillars with spin coated HSQ resist. It is seen that all “balled-up” Ag islands are buried in the HSQ. It should also be noted that AFM analysis has shown that the surface of the HSQ-planarized BPM is very “smooth”, similar to the roughness of the glass substrate prior to planarization. In contrast, the surface of BPM media planarized with sputter-coated SiO_2 tends to yield topography similar to the underlying patterned substrate [74]. After spin-coating, the surplus HSQ is etched back

(Figure 21(b)) by RIE to planarize the surface of the BPM. The time of the RIE process can be controlled to fabricate a nano-topographically manufactured BPM with a desired recess depth. An image of a planarized BPM after back-etching is shown in Figure 21(c). We observe that the trenches are completely filled and that only the Ag masks on the glass pillar are exposed (which in this case serve as simulated protruding magnetic bit islands). If the RIE back etching time is optimized, a BPM design with shallower recess topography can be obtained as shown in Figure 21(d).

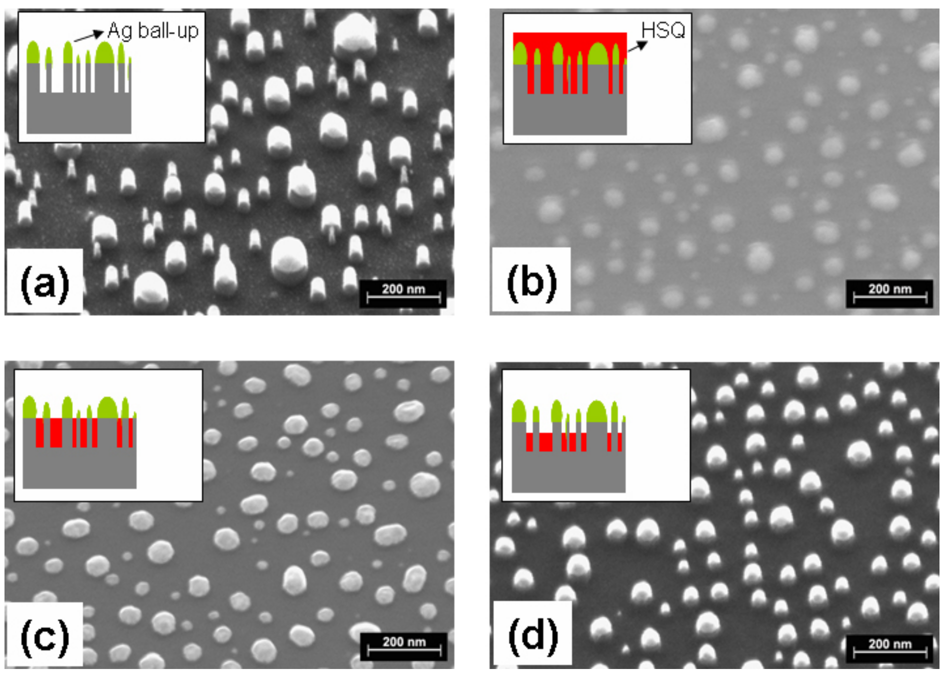

Figure 21. SEM images of (a) patterned pillars with Ag ball-ups, (b) patterned pillars completely filled with HSQ, (c) planarized pillars by RIE etching, and (d) planarized pillars with recess by RIE over-etching. The inset represents a schematic diagram.

Presented in Figure 22 are SEM and AFM images of the BPM media on a Si substrate fabricated by e-beam lithography. Figure 22(a) shows the media before planarization and Figure 22(b) after planarization. The periodicity, diameter and height of the pillars are 100 nm, 40 nm and 40 nm, respectively. As shown in the inset of Fig. 22(a) AFM data, the peak-to-valley height of the as-patterned BPM is measured to be 55 nm. This value is essentially identical to the sum of the height of the glass pillars (40 nm) plus the magnetic layer thickness (15 nm) while the peak-to-valley height measured on the planarized BPM (Figure 22(b)) is 15 nm. Clearly, only the magnetic layer on top of the pillars is exposed.

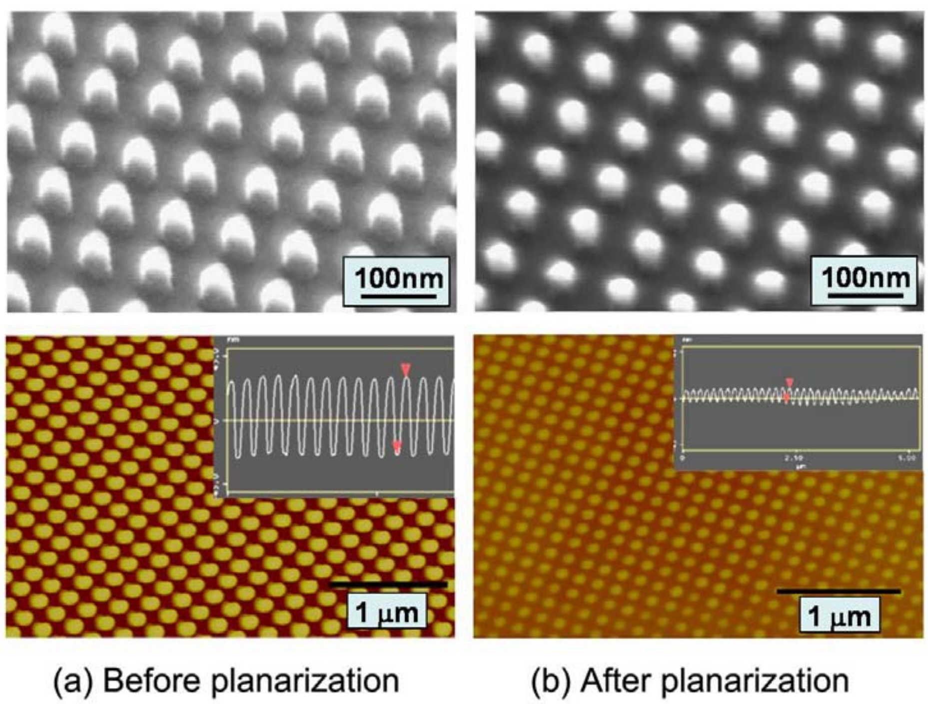

Figure 22. SEM (upper) and AFM (lower) images of (a) before vs (b) after planarization of bit patterned islands. The insets in the AFM images show linescan profiles.

The as-deposited HSQ did not provide sufficient mechanical strength to provide an acceptable tribological interface. It has been reported that the chemical structure of as-spun HSQ exhibits a ladder or cage-like structure which is soft. However, this structure can be transformed into a mechanically stronger, SiO_2-like network structure if HSQ is exposed to oxygen plasma [75-76]. Therefore, prior to the flyability test, we applied oxygen plasma irradiation to harden and densify the planarized HSQ. The BPM structure processed in this way exhibited much better flyability.

To study the flyability of the magnetic recording sliders after planarization, a laser Doppler vibrometer (LDV) was used to measure the flying height fluctuations of the slider on the disk. In this experiment, we used the slider, which was designed to fly at a flying height of 11 nm on a smooth disk at a velocity of 22 m/s. Knigge et al. [77] have investigated the flying height loss of magnetic recording sliders on BPM manufactured with dots of a few micrometer diameters as following equation:

$$\Delta FH = d * \frac{\mathrm{A_r}\ \text{(recessed area)}}{\mathrm{A_t}\ \text{(total area)}} \qquad \text{,where d is the height of a bit}$$

Based on this equation, we roughly estimated the flying height of the sliders on BPM with nano-sized dots; the area ratio of recessed area to total area was found to be 0.45. On a smooth, which is an unpatterned disk, good flyability was observed as shown in Figure 23(a). However, on the unplanarized BPM disk with 40 nm high bits, the slider did not show any flyability. After planarization of the BPM disk, the slider exhibited excellent flying characteristics as is shown in Figure 23(b). In particular, the flying height fluctuations of the slider on the planarized disk are similar to those for a smooth unpatterned media (Figure 23(a)). However, when the depth of the HSQ recess relative to the pillar top surface is intentionally increased to 10 or 20 nm, respectively (e.g., by controlling the degree of RIE etch-back of deposited SiO_2 planarization material), the interactions between slider and disk were found to increase substantially as can be seen from the flying height modulation data shown in Figure 23(c) and (d). The peak to peak values of fluctuations on BPM with recess of 10 nm and 20 nm are increased up to 1 nm and 3 nm, respectively. Figure 24 shows frequency spectra with respect to different planarization conditions. As can be shown in Figure 24 (c), additional frequencies are observed in a range of 30 kHz to 100 kHz, which causes increased fluctuations of the slider. Clearly Figure 24 (d) indicates that severe contacts occurred during flyability test with 20 nm recess on planarized BPM, with a zero expected flying height from estimation with equation (1). These results shows a good agreement with the previous estimated flying height as indicated in Table 1. Table 1 indicates the flying height of sliders with various recess depth after planarization. As is apparent from our study, the planarization of the nanoscale patterned recording media has significantly improved the flyability of the head/disk interface.

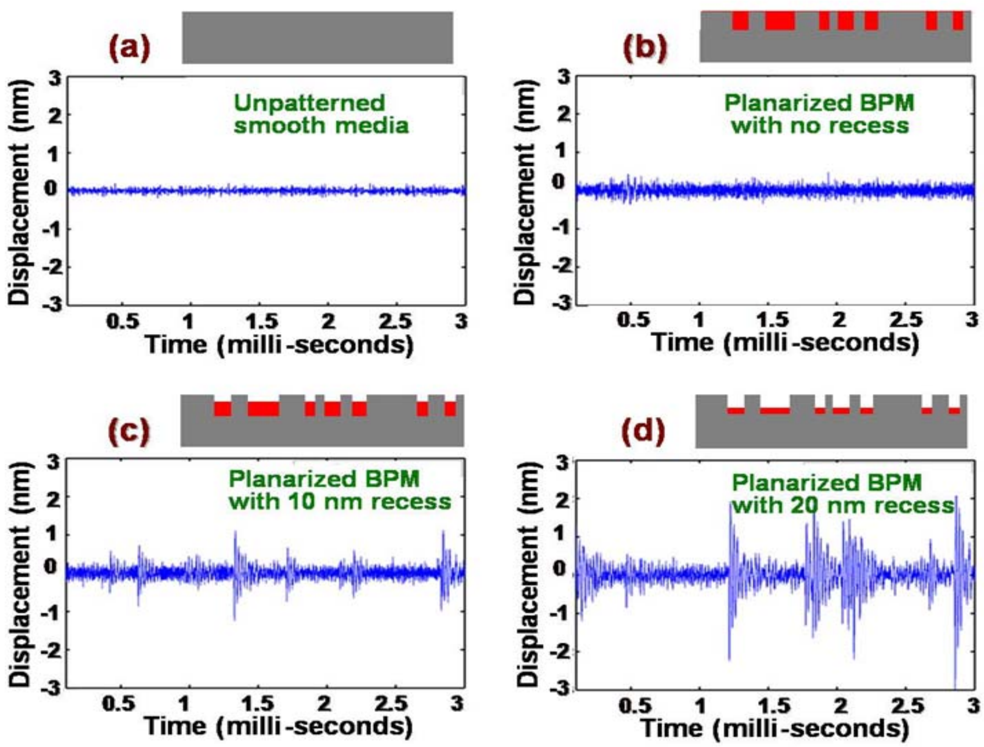

Figure 23. Comparative fluctuation of the flying recording head slider. (a) unpatterned smooth media, (b) planarized BPM with no recess, (c) planarized BPM with 10 nm recess, and (d) planarized BPM with 20 nm recess.

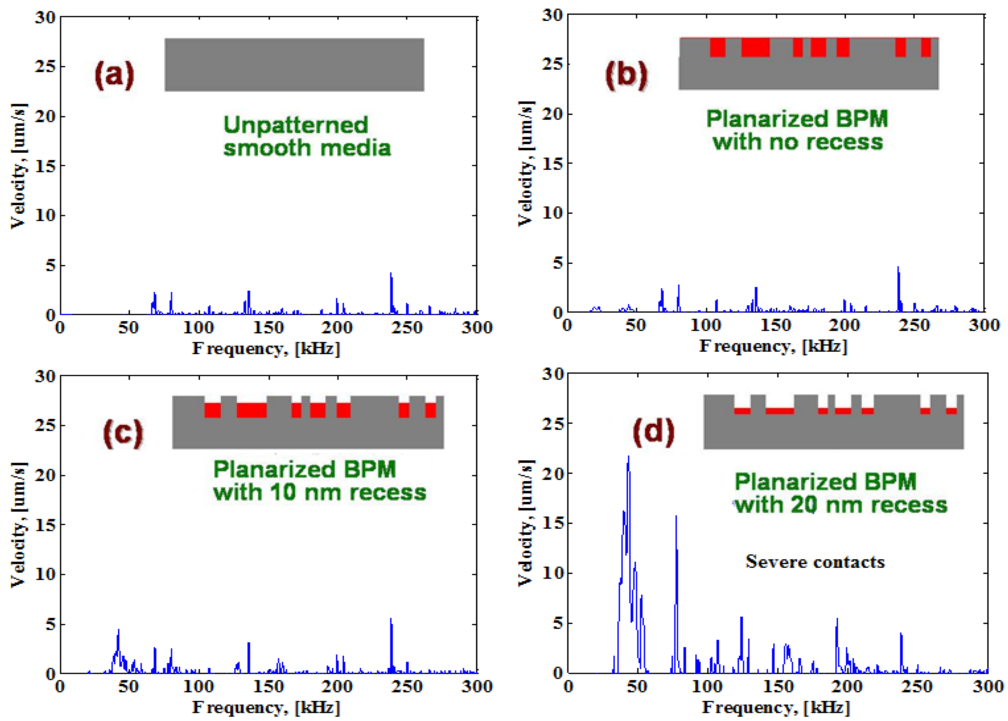

Figure 24. Comparison of frequency spectra (a) on unpatterned smooth disk, (b) on planarized BPM with no recess, (c) on planarized BPM with 10 nm recess, and (d) on planarized BPM with 20 nm recess.

Table 1. Flying height on BPM with various recess depths after planarization

Recess depth (nm)	Flying height (nm)
Zero	11
10	5.5
20	0

3.4 Summary

Nanoscale bit patterned media (BPM) for magnetic hard disk recording have been fabricated by e-beam lithography and RIE process. We have also demonstrated a novel and convenient planarization technique using spin coating of hydrogen silsesquioxane (HSQ) with additional plasma process to mechanically strengthen the HSQ resist, and etch back to expose the magnetic bit pattern for access by read/write flyer head. A large diameter (65 mm) rotatable disk with nano-topographical features was also fabricated using a "balled-up" island array mask and reactive ion etching to simulate the BPM geometry. The recording head flyability was then evaluated for HSQ-planarized disks and compared with disks containing various degrees of topographical protrusions. The HSQ-planarized disk exhibited significantly improved head flyability, similar to that of smooth glass disk surfaces, indicating that the read/write head flyability problem on nano patterned, high-density recording media can be resolved.

This chapter, in full, has been prepared for "Planarization of Patterned Magnetic Recording Media to Enable Head Flyability", (In preparation) by Chulmin Choi, Yeoungching Yoon, Daehoon Hong, Young Oh, Frank E. Talke and Sungho Jin. The dissertation author was the primary investigator and the first author of this paper.

CHAPTER 4: Enhanced Magnetic Properties of Bit Patterned Magnetic Recording Media by Trench-Filled Nanostructure

The structure and properties of, nanoscale magnetic island arrays for BPM were studied, in which the deposition of unwanted magnetic materials outside the island region was prevented by trench-filling. A Si wafer substrate spin-coated with a thin poly-methylmethacrylate (PMMA) layer was nano-imprint-lithography (NIL) processed to form a periodic Si nano-island array. The trench-filling between the protruding Si pillar islands was achieved by PMMA spin coating followed by reactive ion back-etching to remove the overfilled PMMA material beyond the flat surface of the island top. A Co/Pd multilayer magnetic recording media film with a perpendicular anisotropy [Ta 3nm\Pd 3nm\[Co 0.3nm\Pd 0.8nm]$_8$] structure was then sputtered and lifted-off, so that the processed magnetic nanostructure array now has the magnetic material restricted only to the top of pillars. This process significantly improved the magnetic characteristics of the bit patterned media. It is also shown that a SiO_2 filling of the valley regions can be achieved using hydrogen silsesquioxane (HSQ) so as to provide planarization and reduce the tribological interference of the protruding nano-island heights in the bit patterned media.

4.1 Introduction

For hard disk magnetic recording media with substantially improved recording capacity of 1 Terabit/in^2 or higher recording density, a reduction in the feature size or grain size is one of the key requirements [24]. BPM have attracted much attention due to the projected increase in magnetic recording density. Some of the important intrinsic parameters that affect the recording media performance are the thermal stability factor (K_uV/k_BT), proper anisotropy (K_u) and magnetization values with a narrow K_u distribution [7, 55]. Important extrinsic parameters include the uniformity of the nano geometry in the processed patterned media.

It is well known that two major nano-fabrication methods exist for deposition of magnetic material for the patterned media [71, 78-79]. The first approach is the substrate patterning into discrete islands first, followed by magnetic layer deposition. The substrate is pre-patterned into islands using e-beam or nano-imprint lithography before the magnetic material is deposited. The main advantages of this method are that i) no chemical or reactive ion etching process is required for metallic magnetic layer once the substrate island array structure is prepared, ii) and hence the possible damage of the magnetic material associated with ion etching process is minimized, iii) and a high throughput process is possible. However, the magnetic material also deposited in the trenches (between the protruding Si or other substrate islands) can introduce undesirable noises during the read/write process and can cause magnetic interactions between the media material deposited in the trench or island sidewall and that on the top of the islands [78]. The second approach of placing the magnetic layer is to first deposit the high coercivity magnetic thin film material on a flat substrate, then followed by direct patterning of the media layer into discrete magnetic island bits by ion beam etching or focused ion beam milling (FIB). The main advantage of this method is that the magnetic material left between the neighboring bits is minimized to reduce interfering magnetic signals. However, this method has a low throughput with slow etching process for magnetic metal patterning by ion milling, with possible complications of magnetic material re-deposition during the ion-etching process. Also, the magnetic material can more easily be damaged by the ion bombardment required for metal etching [79]. Therefore , a further improved patterning process for magnetic island arrays is desired.

In this work, significantly improved magnetic bit patterned media properties have been obtained by a simple, convenient, and reliable trench-filled nanostructure to ensure the magnetic material deposition only on the patterned media islands. A two-step planarization process of using the PMMA filler first to block the trenches during magnetic layer deposition, followed by HSQ filler to planarize and obtain nano-topographically flat recording media was employed. Both polymers can easily be spin-coated to fill the etched areas.

4.2 Experimental details

Figure 25 schematically illustrates the process used for bit patterned media nanostructure fabrication, trench filler additions and planarization. A Si wafer was spin-coated with an approximately 250 nm thick layer of PMMA (Micro Resist Technology, mr-I 35k PMMA 300). A Si nano imprint stamp (mould) having a nano-hole array (~100 nm diameter and ~150 nm deep holes) is then imprinted onto PMMA layer on Si wafer at ~175^{o}C using an ANT-2 nano imprinter (step (a) in Figure 25). The NIL stamp (mould) was created on (100) silicon wafers by deep ultraviolet (DUV) lithography patterning, reactive ion etch (RIE), and surface oxidation [80]. The NIL patterned PMMA was slightly RIE etched (Oxford Plasmalab-80) in a gas mixture of CF_4 and O_2 to form a through hole (Figure 25(c)). The hole-patterned PMMA was then used as an etching mask for Si etching to faithfully transfer the patterns into Si wafer using a mixture of SF_6 and C_4F_8 for RIE (Oxford Plasmalab-100) as illustrated in Figure 25(d), followed by removal of PMMA by O_2 plasma to produce an array of protruding Si nano island columns (~100 nm diameter and ~150 nm tall), Figure 25(e).

In order to place the magnetic bit layer only on top of pillars, we utilized a nanoscale filling and manipulation of the Figure 25(e) nanostructured substrate as illustrated by the insets in Figure 26(c). A thin PMMA layer was first spin coated to fill the valley and subsequently re-etched by a CF_4 and O_2 mixture RIE to remove the overfilled regions on the substrate for planarization. A magnetically hard Co/Pd multilayer film, having a [Ta 3nm\Pd 3nm\[Co 0.3nm\Pd 0.8nm]$_8$ structure with desirable perpendicular magnetic anisotropy was sputtered on the pre-patterned and planarized substrate.

After magnetic layer deposition, the filling processed BPM was lifted-off by acetone and sonication. A HSQ (hydrogen silsesquioxane resist, Dow Corning No. Fox-13) film was spun on the BPM to fill the trenches and subsequently back-etched by RIE to remove the “overfilled” extra HSQ material. The surface roughness of the nanostructured BPM before vs. after trench filling was monitored by atomic force microscopy (AFM) and scanning electron microscopy (SEM). The magnetic properties of the BPM media material were evaluated by magnetic force microscopy (MFM) and superconducting quantum interference device (SQUID) with vs. without the trench-filled nanostructure.

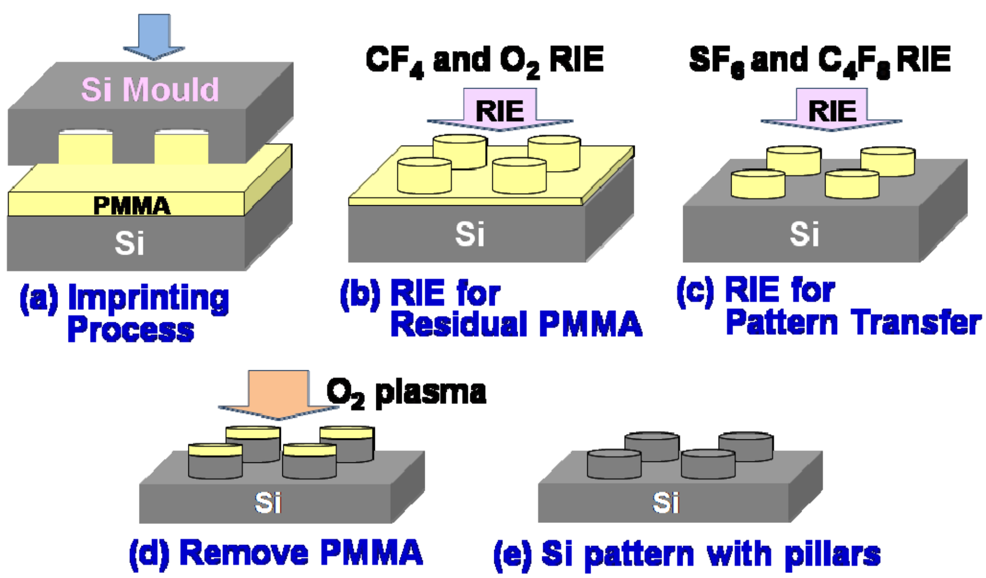

Figure 25. Schematic illustration of the fabrication processes for bit patterned media (BPM) using trench-filling process.

4.3 Results and Discussion

As a demonstration of principle, we fabricated a ~100 nm diameter periodic array of Si nano pillars using nano imprint lithography (NIL). Each of the samples contained ~100 million Si nano pillars over a relatively large area of 0.6 cm x 0.6 cm. The oblique angle SEM image of the bit patterned media consisting of high-coercivity magnetic multilayer stacks of [Ta 3 nm\Pd 3 nm\[Co 0.3 nm\Pd 0.8 nm]$_8$] deposited on top of Si islands as well as in the valleys (trenches) is shown in Figure 26(a). Our patterned Si islands have a dimension of ~100 nm diameter, ~150 nm heights and a periodicity of 400 nm. It is also found that the phase of bit pattern is uniform, which is related to the Si substrate patterning. It is notable that the Si island nano feature dimension is undesirably altered during the magnetic multilayer deposition, with the magnetic materials deposited in the trench, on the top, as well as on the sidewall of the pillars. Also shown in Figure 26(b) is the SEM image of the Figure 26(a) nano pillar structure subjected to an additional process of geometrical planarization using HSQ (hydrogen silsesquioxane) spin coating, back etch and conversion of the trench HSQ into SiO_2 by the plasma treatment. The trenches are completely filled by HSQ. The planarization process has reduced the bit height from ~150 nm to flat, 15 nm layer. Only the magnetic bit islands are exposed.

In order to restrict the presence of magnetic materials only on the pillar top, not in the unwanted places such as sidewall and valley, the samples were pre-covered by PMMA (poly-methylmethacrylate) using spin coating before magnetic layer deposition so as to exclude the magnetic materials on these unwanted locations. After spin coating, the superfluous PMMA is back-etched by RIE to reveal the top of the Si islands. The required RIE time depends on the thickness of PMMA, the height of the Si pillars, and the etching rate. A SEM image of a BPM with the magnetic recording media material restricted to the Si pillar top area via the trench-filling process is shown in Figure 26(c). It is apparent that the trench filled nano structure controls the location of magnetic material in a well-defined manner and prevents the unwanted deposition of magnetic material outside the pillar tip region.

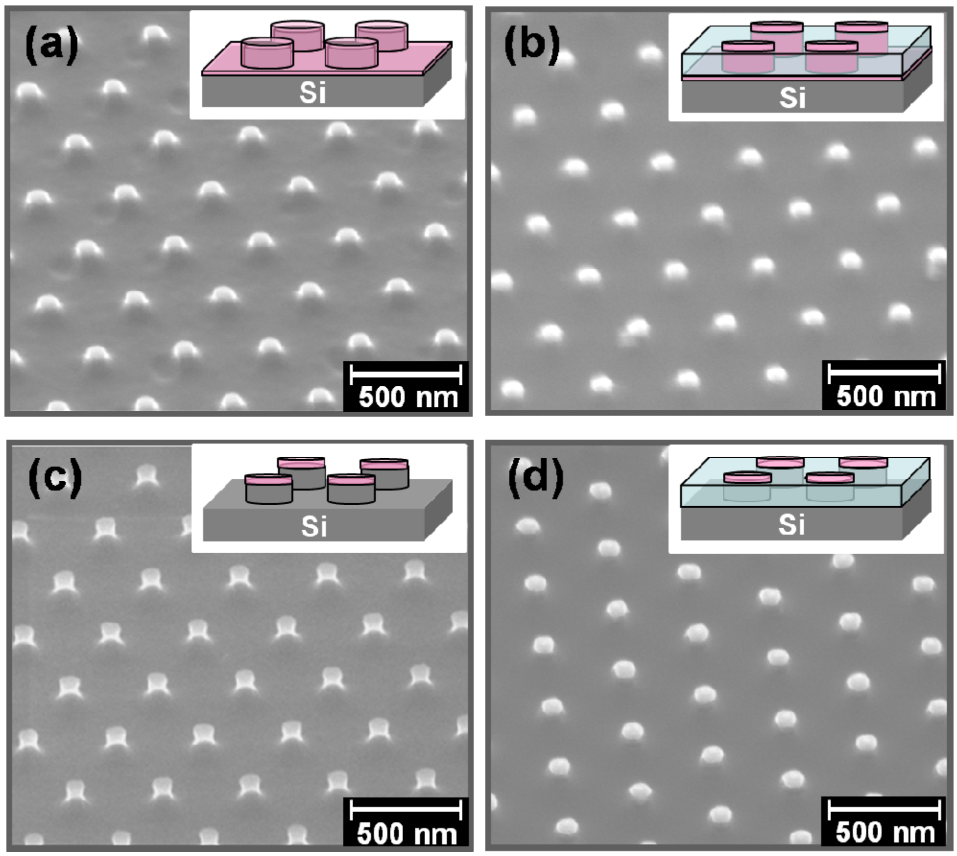

Figure 26. SEM images showing topographical features of bit patterned media. (a) magnetic media deposited without trench filling, (b) the structure of (a) + additional geometry planarization, (c) magnetic media deposited with trench filling for isolated magnetic islands, and (d) the structure of (c) + additional geometry planarization. The insets show the schematic description of the BPM nanostructures.

To evaluate how such nano structural manipulations influence the magnetic behavior of BPM media, the magnetic properties of BPM were measured and analyzed. Figure 27(a) shows the M-H magnetization loop of the patterned media measured by SQUID (superconducting quantum interference device), without the trench filling process. This M-H loop appears to have two distinctly different regions. The Region A (marked in Figure 27(a)) represents the magnetic signal from the relatively continuous CoPd multilayer film in the valley, which exhibits a low coercivity of only about 600 Oe as anticipated for non-nanosize Co-Pd layer materials. The Region B, on the other hand, shows the magnetic signal from the ~100 nm diameter size-confined CoPd multilayer islands on top of the Si pillars, which exhibits a much higher coercivity of about 5000 Oe. It was known that the smaller CoPd multilayer islands produce much higher coecivity. The M-H loop clearly shows that not only was the magnetic multi layer present on top of pillars, but on sidewall and valley. Shown in of Figure 27(b) is the M-H loop measured from BPM with magnetic material confined to the Si pillar top only, accomplished by using the trench-filling process. Contrary to the M-H loop of Fig. 27(a) for the BPM without filling process, the Figure 27(b) exhibits a much better defined M-H loop indicative of a more uniform material, namely only the pillar top island magnetic material.

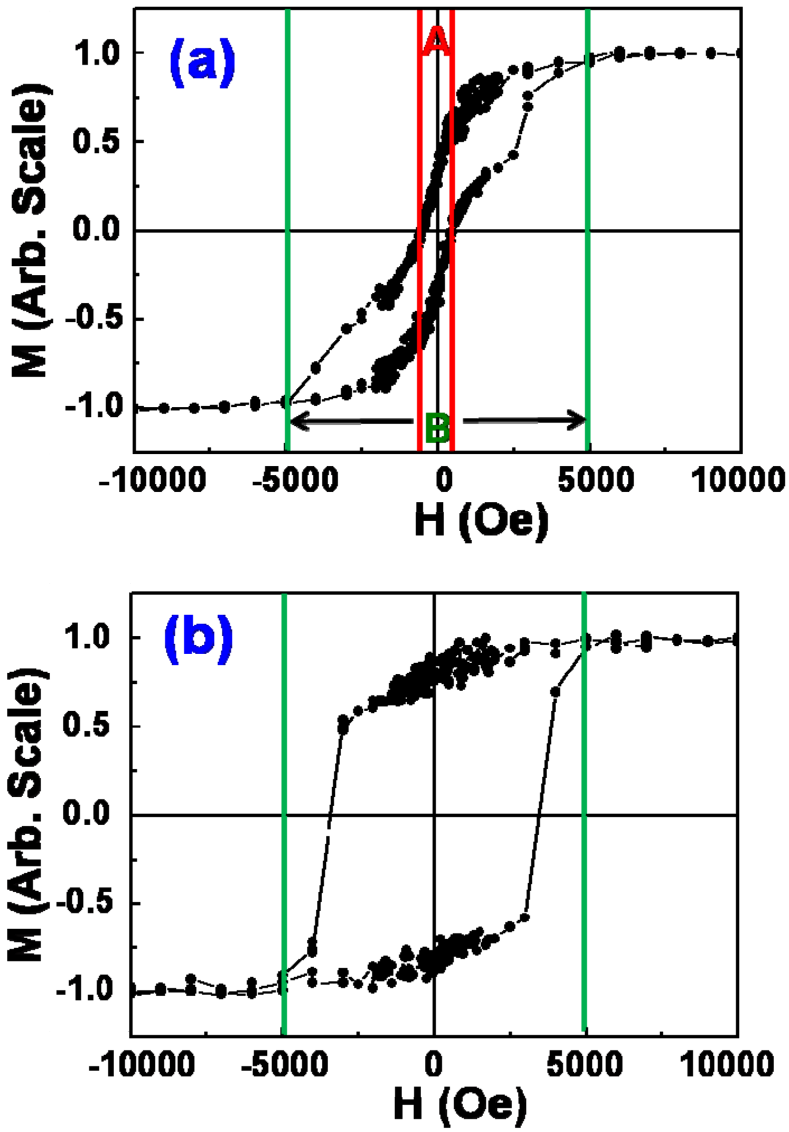

Figure 27. M-H loop of bit patterned media by SQUID measurements for (a) BPM with unremoved magnetic materials in the trenches, (b) BPM with trench filling process for isolated magnetic islands.

Shown in Figure 28(a) are typical magnetic force microscopy (MFM) & atomic force microscopy (AFM) images of the BPM without the filling process. The schematics in the insets illustrate the cross-sectional geometry of the magnetic recording media in relation to the substrate and the HSQ filler material. The AFM data, Figure 28(a) (rightside image, representing ~5 μm square area) indicates a relatively uniform pillar array. The MFM image (leftside image) shows a somewhat smaller island images, which is possibly related to the larger measurement distance between MFM probe tip and magnetic multilayer surface as compared to the AFM imaging. The light phase vs. dark phase represent opposite magnetization direction in the MFM imaging. It is seen that the valley regions also show some response to the MFM imaging (darker and blurry contrast regions) indicating the presence of magnetic materials in the valley. In the BPM processed with the trench-filling step (thus having the magnetic material only on the island top), the MFM image of Figure 28(b) leftside is much more uniform than the case of Figure 28(a) MFM imaging, and exhibits no dark contrast regions from the valley seen in Figure 28(a).

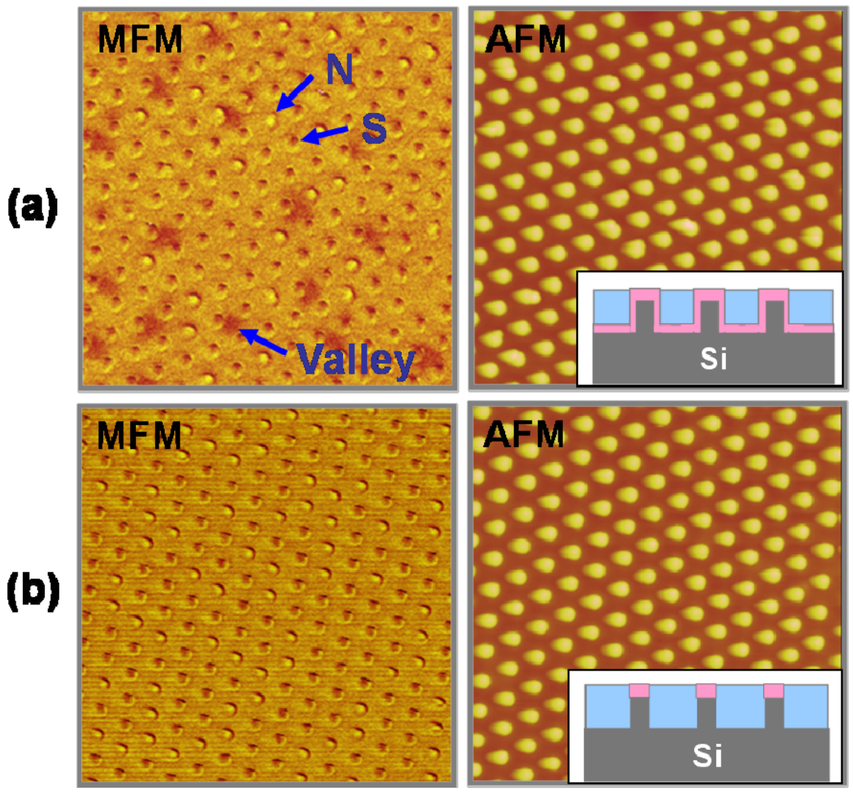

Figure 28. MFM data (left) and AFM data (right) of BPM (a) without trench filling process vs. (b) with trench filling process.

Higher resolution MFM image of the BPM with the filling process (magnetic material only on the pillar top), Figure 29, indicates further details of the domain structure. Because of the somewhat larger island diameter of ~100 nm, the magnetic island is not a single domain in this particular case, and a two-domain structure is therefore observed. It is anticipated that a single domain structure in a periodic arrangement will be obtained if the island diameter is reduced to ~50 nm or smaller, which is one of the current research topics at UCSD.

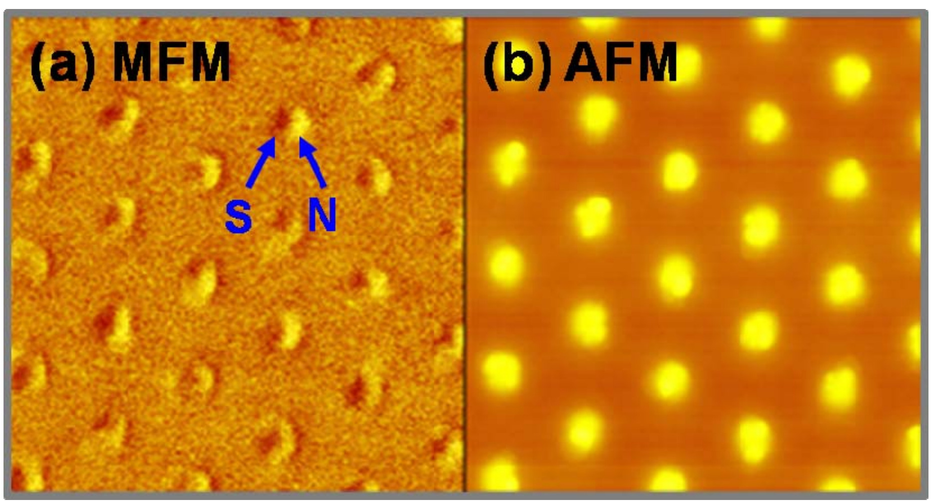

Figure 29. Higher resolution images of (a) MFM and (b) AFM for the BPM with trench filled nanostructure.

4.4 Summary

The structure and properties of nano scale magnetic island arrays with different size, geometry and configurations were investigated for bit patterned media (BPM). Modifications of the patterned media configuration in which the deposition of unwanted magnetic materials outside the island region was prevented by trench-filling was also demonstrated. A Co-Pd multilayer magnetic media layer placed on nano-imprint-lithography processed, periodic Si nano-island array using such trench-filling steps exhibited significantly improved magnetic characteristics of the bit patterned media, as well as the flyability of recording read/write head off the magnetic disk surface.

This chapter, in full, has been prepared for “Enhanced Magnetic Properties of Bit Patterned Magnetic Recording Media by Trench-Filled Nanostructure”, (In preparation) by Chulmin Choi, Daehoon Hong, Young Oh, Leon Chen, Sy-Hwang Liou and Sungho Jin. The dissertation author was the primary investigator and the first author of this paper.

CHAPTER 5: Effect of Magnetic Island Geometry on Switching Field Distribution

In addition to the fabrication of the nano-array patterned structure and planarization aspects, there is also an issue of magnetic switching field distribution (SFD) in the patterned recording media. For hard disk media switching of magnetic polarity (writing), it is important that the magnetic switching of various island bits occur at a consistent and same applied magnetic field. In reality, patterned media have some distribution of switching field due to various microstructural and compositional and geometrical variations among the magnetic bit islands.

When the bit size is on the order of 10 nm, a small variation of e.g., 1 nm in the island diameter can induce a significant change in the magnetic volume, coercivity and switching field. The deposition of magnetic island on top of the silicon pillar top can also be nonuniform, for example, any unwanted deposition of magnetic materials on the sidewall of Si pillar or at the corners/edges of the pillar top and pillar side wall.

To operate the magnetic hard disk drive memory, the recorded bits need to be switched between “1” vs “0” (which is typically obtained by changing of magnetization directions through north pole - south pole switching. The desired magnetic field for switching of recorded bits in future high-density hard disk drive is typically ~5 – 10 KOe. Recent literatures report a substantial undesirable variation of the magnetic switching field when the size of the magnetic nano islands is reduced to below ~ 50 nm.

The switching field distribution is sometimes more than 30% from the median coercive force value, which is unacceptable from the hard disk memory application point of view. Various possible causes were discussed --- dimensional variations after lithographic patterning, islands sizes variations, islands edge effects, local compositional variation of Co and Pd at interfaces of the $(Co/Pd)_n$ superlattice recording media, distribution of intrinsic magnetic anisotropy, grain orientation and sizes or grain boundary variations.

Understanding of why such a switching field variation occurs in nanoscale dimensions and how to prevent such a phenomenon are of paramount issue that has to be resolved for developing the ultra-high-density magnetic recording media so that the switching of bit information is carried out in a reproducible manner. While some of the recent literature report that the distribution of intrinsic magnetic anisotropy might be the cause for the switching field variation, there are additional possibilities for the cause of the SFD (switching field distribution) that have not been addressed. One of these possibilities includes the fact that the shape of nano-magnet islands fabricated by e-beam lithography is not always uniform. Depending on the shape of the substrate Si pillars (vertical, positively tapered, or negatively tapered) as illustrated in Fig. 30, there can be some sidewall deposition of magnetic recording media, which can contribute to the observed SFD.

As the magnetic layer deposition on top of protruding pillars tends to have some corner and sidewall deposition, this may cause different magnetic properties and switching fields, and may cause SFD in the magnetic islands. To investigate if a removal of such sidewall deposition reduces the SFD problem, the RIE parameters have been intentionally modified so as to alter the shape of the sidewall in Si nanopillars and introduced negative tapered Si column geometry as illustrated in Fig. 30. The figure shows ~30-50 nm diameter Si islands having the three different sidewall configurations, fabricated by e-beam lithography utilizing various RIE conditions.

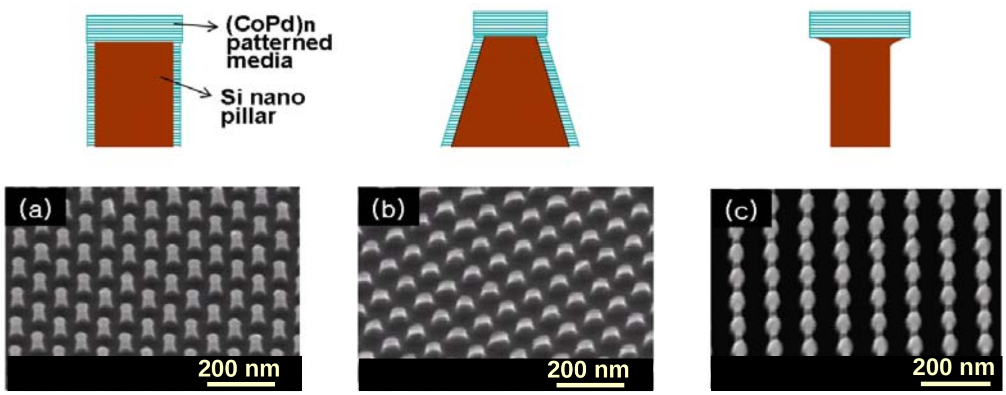

Figure 30. Control of Si pillar sidewall configurations.

Based on reproducible Si nano-island array preparation, patterned magnetic recording media have been fabricated as described in Fig. 31. About ~30 nm diameter Si pillar array was fabricated by E-beam lithography patterning as the basis to deposit magnetic material. High coercive force magnetic layer of multilayered magnet of $(Co/Pd)_n$ [n=8] with strong perpendicular magnetic anisotropy was sputter deposited on the top surface of Si pillars. The structured multilayer nanomagnets also consist of other adhesion layer and anisotropy-inducing layer by utilizing the geometry of Ta 3 nm\Pd 3 nm\[Co 0.3

nm\Pd 0.8 nm]$_8$. The coercivity was Hc ~4 KOe. (If a FePt (L1o phase) islands are sputter deposited, a higher Hc of ~15KOe expected.)

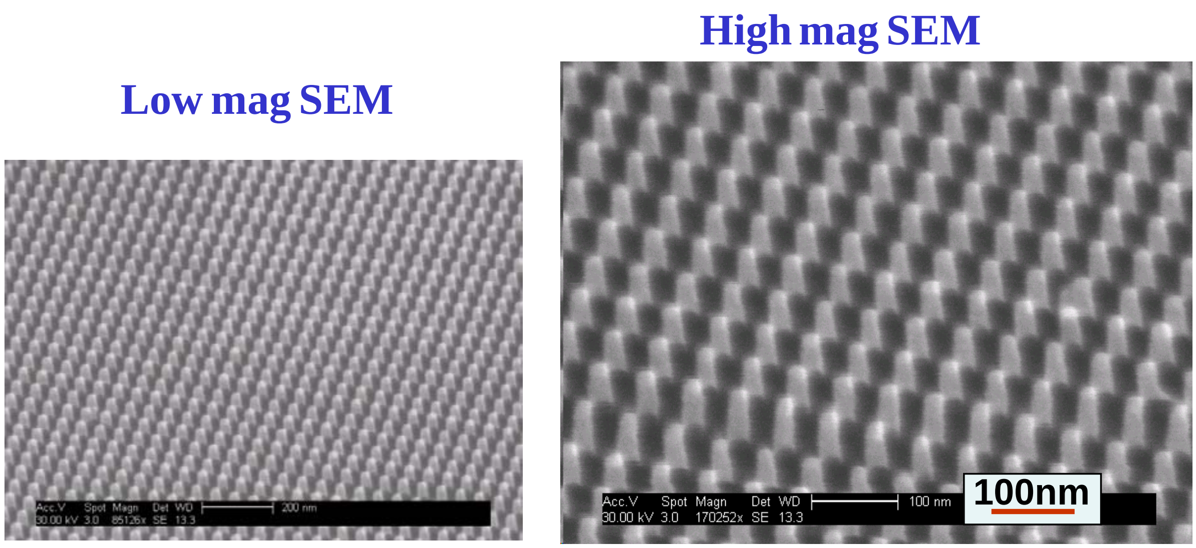

Figure 31. Patterned magnetic recording media fabricated. The $[CoPd]_n$ islands with n=8 (~30 nm regime) were sputter deposited on Si nano pillars.

Comparative magnetic properties of patterned media islads with different sidewall configuration were evaluated using Micro MOKE measurements. As shown in Fig. 32 for the second quadrant M-H loop, the measurement data clearly indicates that the magnetic coercivity of $[Co/Pd]_n$ islands (~30 nm regime) on Si nano pillars with vertical sidewall has less variation in coercivity of ~15.3% in the switching field distribution (SFD) than that with positive side wall (~20.3%). Therefore it has been shown that the slanted geometry of the patterned media magnetic islands is less desirable than vertical wall geometry. The magnetic measurement for the negative slope geometry sample would minimize the deposition of the magnetic material on the sidewall of the Si pillar, which is likely to further reduce the SFD. Such experiments are in progress.

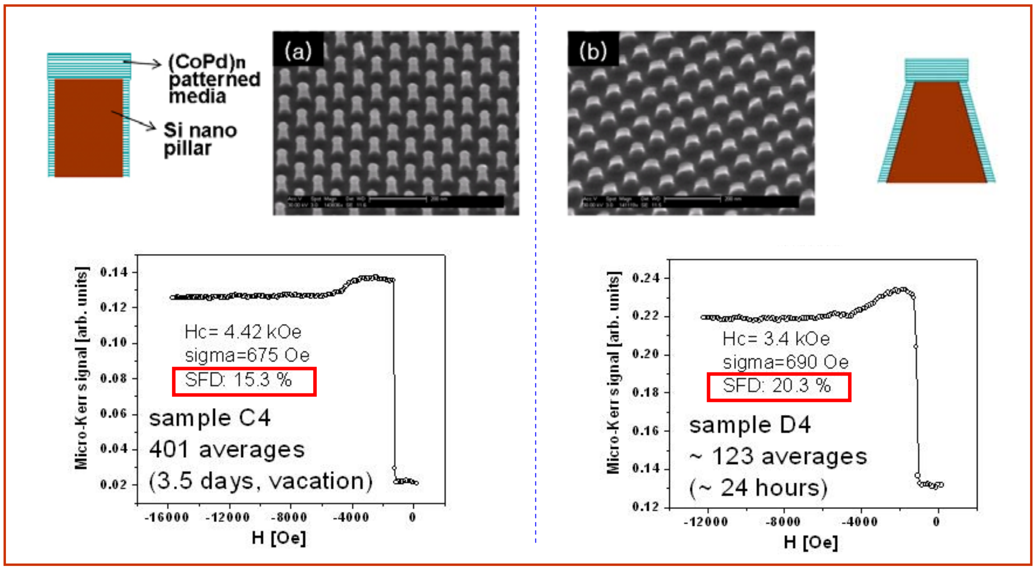

Figure 32. Micro MOKE measurements of M-H loop for the patterned magnetic recording media, with the structured multilayer magnet of Ta 3 nm\Pd 3 nm\[Co 0.3 nm\Pd 0.8 nm]$_8$ sputter deposited on Si nano pillars.

CHAPTER 6: Summary, Conclusions, and Future Work

In summary, the Si nanopillars have been prepared by electron beam lithography (EBL) and reactive ion etching (RIE). The diameter and pitch of the patterned pillars are sensitively affected by the properties of electron beam resist and developer combination and pattern transfer. In this work, poly-methylmethacrylate (PMMA), Calixarene, and hydrogen silsesquioxane (HSQ) have been studied in terms of the nanofabrication control of magnetic island geometry, and microstructural, magnetc and mechanical properties. HSQ resist has some advantages over PMMA and Calixarene because it is relatively robust against RIE plasma and ion bombardment. To satisfy high density magnetic storage, we are exploring an EBL process with thin HSQ resist using diluted BOE development. The smallest island size and pitch of the nano-patterned Si arrays we were able to demonstrate was sub 10 nm and sub 20 nm with HSQ. It corresponds to a high areal density of 1.6 Terabit/inch^2.

Second, we have fabricated nanoscale bit patterned media (BPM) by e-beam lithography and RIE process for pattern transfer from the resist nanopattern to Si and 10 nm diameter magnetic nanopattern, with the magnetic island bit density as high as 1.6 Terabit/inch^2. We have also demonstrated a novel and convenient planarization technique using spin coating of hydrogen silsesquioxane (HSQ), plasma process to mechanically strengthen the HSQ resist, and etch back to expose the magnetic bit pattern for access by read/write flyer head. A large diameter (65 mm) rotatable disk with nano-topographical features was also fabricated using a “balled-up” island array mask and reactive ion etching to simulate the BPM geometry. The recording head flyability was then evaluated for HSQ-planarized disks and compared with disks containing various degrees of topographical protrusions. The HSQ-planarized disk exhibited significantly improved head flyability, similar to that of smooth glass disk surfaces, indicating that the read/write head flyability problem on nano patterned, high-density recording media can be resolved.

It has also been demonstrated that the magnetic island geometry influences the switching field distribution (SFD). A magnetic island of $(CoPd)_n$ superlattice having a slanted surface is shown to exhibit more severe SFD than a vertical sidewalled pillar geometry, which points to a need to control the Si/magnetic island pillar shape in addition to the pillar dimension.

Finally, the process, structure and magnetic properties of planarized vs. non-planarized nano fabricated and nano-imprinted bit patterned media, has been onvestigated. A Si wafer substrate was spin-coated with a thin PMMA layer, and a periodic island array bit pattern was made by nano-imprinting lithography (NIL) with the patterned nanofeatures. The subsequent pattern transfer to the Si substrate was performed by using reactive ion etching (RIE). A magnetically hard Co/Pd multilayer film with {Ta 3nm\Pd 3nm\[Co 0.3nm\Pd 0.8nm]$_8$} structure was sputtered on the pre-patterned substrate. A thin HSQ layer was first spin coated on the patterned media to fill the “trenches” and subsequently re-etched by RIE to remove the “overfilled” regions on the substrate for planarization. Periodic Si nano-island array using such trench-filling steps provided a well defined and clean magnetic island configuration with no undesirable magnetic material present between adjacent bit islands, and hence exhibited significantly improved magnetic characteristics of the bit patterned media.

The patterning of magnetic domains requires industrial-scale lithography at unprecedented levels of feature resolution, pattern precision, and cost efficiency. Recent trends in recording media research indicate that the use of templated self-assembly for nanolithography (for example, di-block copolymers and various other nanomaterials processes) offers interesting possibilities for improved and possibly practical patterned media although many issues and challenges remain to be resolved to realize the next generation of hard-disk drives with storage densities exceeding 1 Terabit/inch^2.

REFERENCES

1. Kittel, C., THEORY OF THE STRUCTURE OF FERROMAGNETIC DOMAINS IN FILMS AND SMALL PARTICLES. Physical Review, 1946. 70(11-1): p. 965-971.

2. Neel, L., INFLUENCE DES FLUCTUATIONS THERMIQUES SUR LAIMANTATION DE GRAINS FERROMAGNETIQUES TRES FINS. Comptes Rendus Hebdomadaires Des Seances De L Academie Des Sciences, 1949. 228(8): p. 664-666.

3. Stoner, E.C. and E.P. Wohlfarth, A MECHANISM OF MAGNETIC HYSTERESIS IN HETEROGENEOUS ALLOYS. Philosophical Transactions of the Royal Society of London Series a-Mathematical and Physical Sciences, 1948. 240(826): p. 599-642.

4. Lu, L., M.L. Sui, and K. Lu, Superplastic extensibility of nanocrystalline copper at room temperature. Science, 2000. 287(5457): p. 1463-1466.

5. Weller, D. and A. Moser, Thermal effect limits in ultrahigh-density magnetic recording. Ieee Transactions on Magnetics, 1999. 35(6): p. 4423-4439.

6. Brown, W.F., THERMAL FLUCTUATIONS OF A SINGLE-DOMAIN PARTICLE. Physical Review, 1963. 130(5): p. 1677-&.

7. Charap, S.H., P.L. Lu, and Y.J. He, Thermal stability of recorded information at high densities. Ieee Transactions on Magnetics, 1997. 33(1): p. 978-983.

8. Bertram, H.N. and M. Williams, SNR and density limit estimates: A comparison of longitudinal and perpendicular recording. Ieee Transactions on Magnetics, 2000. 36(1): p. 4-9.

9. Web Resource, H.G.S.T., http://www.hitachigst.com/tech/techlib.nsf/techdocs/F47BF010A4D29DFD8625716C005B7F34/$file/PMR_white_paper_final.pdf.

10. Web Resource, H.G.S.T., http://www.hitachigst.com/hdd/research/recording_head/pr/PerpendicularPaper.html.

11. Web Resource, H.G.S.T., http://www.hitachigst.com/hdd/research/storage/pm/index.html.

12. Chou, S.Y., et al., STUDY OF NANOSCALE MAGNETIC-STRUCTURES FABRICATED USING ELECTRON-BEAM LITHOGRAPHY AND QUANTUM MAGNETIC DISK. Journal of Vacuum Science & Technology B, 1994. 12(6): p. 3695-3698.

13. Chou, S.Y., Patterned magnetic nanostructures and quantized magnetic disks. Proceedings of the Ieee, 1997. 85(4): p. 652-671.

14. White, R.L., R.M.H. New, and R.F.W. Pease, Patterned media: A viable route to 50 Gbit/in(2) and up for magnetic recording? Ieee Transactions on Magnetics, 1997. 33(1): p. 990-995.

15. Bandic, Z.Z. and R.H. Victora, Advances in Magnetic Data Storage Technologies. Proceedings of the Ieee, 2008. 96(11): p. 1749-1753.

16. Hintz, M.B., A HYBRID RECORDING SCHEME FOR HIGH-AREAL-DENSITY INFORMATION-STORAGE. Journal of Applied Physics, 1991. 69(8): p. 5767-5767.

17. Ruigrok, J.J.M., et al., Disk recording beyond 100 Gb/in.(2): Hybrid recording? (invited). Journal of Applied Physics, 2000. 87(9): p. 5398-5403.

18. Alex, M., et al., Characteristics of thermally assisted magnetic recording. Ieee Transactions on Magnetics, 2001. 37(4): p. 1244-1249.

19. Moser, A., et al., Magnetic recording: advancing into the future. Journal of Physics D-Applied Physics, 2002. 35(19): p. R157-R167.

20. McDaniel, T.W., W.A. Challener, and K. Sendur, Issues in heat-assisted perpendicular recording. Ieee Transactions on Magnetics, 2003. 39(4): p. 1972-1979.

21. Hamann, H.F., Y.C. Martin, and H.K. Wickramasinghe, Thermally assisted recording beyond traditional limits. Applied Physics Letters, 2004. 84(5): p. 810-812.

22. Challener, W.A., et al., Heat-assisted magnetic recording by a near-field transducer with efficient optical energy transfer (vol 3, pg 220, 2009). Nature Photonics, 2009. 3(5): p. 303-303.

23. Rousseau, E., et al., Radiative heat transfer at the nanoscale. Nature Photonics, 2009. 3(9): p. 514-517.

24. Victora, R.H., J.H. Xue, and M. Patwari, Areal density limits for perpendicular magnetic recording. Ieee Transactions on Magnetics, 2002. 38(5): p. 1886-1891.

25. Victora, R.H. and X. Shen, Exchange coupled composite media for perpendicular magnetic recording. Ieee Transactions on Magnetics, 2005. 41(10): p. 2828-2833.

26. Wang, J.P., W.K. Shen, and J.M. Bai, Exchange coupled composite media for perpendicular magnetic recording. Ieee Transactions on Magnetics, 2005. 41(10): p. 3181-3186.

27. Wang, J.P., W.K. Shen, and S.Y. Hong, Fabrication and characterization of exchange coupled composite media. Ieee Transactions on Magnetics, 2007. 43(2): p. 682-686.

28. Victora, R.H. and X. Shen, Exchange Coupled Composite Media. Proceedings of the Ieee, 2008. 96(11): p. 1799-1809.

29. Tang, Y.H., et al., Optimization of perpendicular recording on exchange coupled composite media. Journal of Applied Physics, 2008. 103(7).

30. Lodder, J.C., Methods for preparing patterned media for high-density recording. Journal of Magnetism and Magnetic Materials, 2004. 272: p. 1692-1697.

31. Terris, B.D., T. Thomson, and G. Hu, Patterned media for future magnetic data storage. Microsystem Technologies-Micro-and Nanosystems-Information Storage and Processing Systems, 2007. 13(2): p. 189-196.

32. Bandic, Z.Z., et al., Patterned magnetic media: impact of nanoscale - Patterning on hard disk drives. Solid State Technology, 2006: p. S7-+.

33. Pfeiffer, H.C., T.R. Groves, and T.H. Newman, HIGH-THROUGHPUT, HIGH-RESOLUTION ELECTRON-BEAM LITHOGRAPHY. Ibm Journal of Research and Development, 1988. 32(4): p. 494-501.

34. Chang, T.H.P., et al., Electron-beam microcolumns for lithography and related applications. Journal of Vacuum Science & Technology B, 1996. 14(6): p. 3774-3781.

35. Grigorescu, A.E. and C.W. Hagen, Resists for sub-20-nm electron beam lithography with a focus on HSQ: state of the art. Nanotechnology, 2009. 20(29).

36. Guo, L.J., Nanoimprint lithography: Methods and material requirements. Advanced Materials, 2007. 19(4): p. 495-513.

37. Chou, S.Y., P.R. Krauss, and P.J. Renstrom, Imprint lithography with 25-nanometer resolution. Science, 1996. 272(5258): p. 85-87.

38. Bates, F.S., POLYMER-POLYMER PHASE-BEHAVIOR. Science, 1991. 251(4996): p. 898-905.

39. Fredrickson, G.H. and F.S. Bates, Dynamics of block copolymers: Theory and experiment. Annual Review of Materials Science, 1996. 26: p. 501-550.

40. Thomas, E.L. and R.L. Lescanec, PHASE MORPHOLOGY IN BLOCK-COPOLYMER SYSTEMS. Philosophical Transactions of the Royal Society of London Series a-Mathematical Physical and Engineering Sciences, 1994. 348(1686): p. 149-166.

41. Bita, I., et al., Graphoepitaxy of self-assembled block copolymers on two-dimensional periodic patterned templates. Science, 2008. 321(5891): p. 939-943.

42. Yang, J.K.W., et al., Complex self-assembled patterns using sparse commensurate templates with locally varying motifs. Nature Nanotechnology, 2010. 5(4): p. 256-260.

43. Hawker, C.J. and T.P. Russell, Block copolymer lithography: Merging "bottom-up" with "top-down" processes. Mrs Bulletin, 2005. 30(12): p. 952-966.

44. Ruiz, R., et al., Density multiplication and improved lithography by directed block copolymer assembly. Science, 2008. 321(5891): p. 936-939.

45. Tang, C.B., et al., Evolution of block copolymer lithography to highly ordered square arrays. Science, 2008. 322(5900): p. 429-432.

46. Chuang, V.P., et al., Three-dimensional self-assembly of spherical block copolymer domains into V-shaped grooves. Nano Letters, 2006. 6(10): p. 2332-2337.

47. Cheng, J.Y., A.M. Mayes, and C.A. Ross, Nanostructure engineering by templated self-assembly of block copolymers. Nature Materials, 2004. 3(11): p. 823-828.

48. Jung, Y.S., W. Jung, and C.A. Ross, Nanofabricated concentric ring structures by templated self-assembly of a diblock copolymer. Nano Letters, 2008. 8(9): p. 2975-2981.

49. Chuang, V.P., et al., Self-Assembled Nanoscale Ring Arrays from a Polystyrene-b-polyferrocenylsilane-b-poly(2-vinylpyridine) Triblock Terpolymer Thin Film. Advanced Materials, 2009. 21(37): p. 3789-3793.

50. Chuang, V.P., et al., Templated Self-Assembly of Square Symmetry Arrays from an ABC Triblock Terpolymer. Nano Letters, 2009. 9(12): p. 4364-4369.

51. Klein, D.L., et al., A single-electron transistor made from a cadmium selenide nanocrystal. Nature, 1997. 389(6652): p. 699-701.

52. Simon, U., Charge transport in nanoparticle arrangements. Advanced Materials, 1998. 10(17): p. 1487-1492.

53. Joannopoulos, J.D., P.R. Villeneuve, and S.H. Fan, Photonic crystals: Putting a new twist on light. Nature, 1997. 386(6621): p. 143-149.

54. Liu, X.G., et al., Arrays of magnetic nanoparticles patterned via "dip-pen" nanolithography. Advanced Materials, 2002. 14(3): p. 231-+.

55. Terris, B.D. and T. Thomson, Nanofabricated and self-assembled magnetic structures as data storage media. Journal of Physics D-Applied Physics, 2005. 38(12): p. R199-R222.

56. Chou, S.Y., et al., SINGLE-DOMAIN MAGNETIC PILLAR ARRAY OF 35-NM DIAMETER AND 65-GBITS/IN(2) DENSITY FOR ULTRAHIGH DENSITY QUANTUM MAGNETIC STORAGE. Journal of Applied Physics, 1994. 76(10): p. 6673-6675.

57. Naito, K., et al., 2.5-inch disk patterned media prepared by an artificially assisted self-assembling method. Ieee Transactions on Magnetics, 2002. 38(5): p. 1949-1951.

58. Gapin, A.I., et al., Patterned media based on soft/hard composite nanowire array of Ni/CoPt. Ieee Transactions on Magnetics, 2007. 43(6): p. 2151-2153.

59. Jeong, J.R., et al., Fabrication of hexagonal lattice Co/Pd multilayer nanodot Arrays using colloidal lithography. Small, 2007. 3(9): p. 1529-1533.

60. Ross, C.A., et al., Fabrication of patterned media for high density magnetic storage. Journal of Vacuum Science & Technology B, 1999. 17(6): p. 3168-3176.

61. Turchanin, A., et al., Fabrication of molecular nanotemplates in self-assembled monolayers by extreme-ultraviolet-induced chemical lithography. Small, 2007. 3(12): p. 2114-2119.

62. Solak, H.H. and Y. Ekinci, Bit-array patterns with density over 1 Tbit/in.(2) fabricated by extreme ultraviolet interference lithography. Journal of Vacuum Science & Technology B, 2007. 25(6): p. 2123-2126.

63. Hosaka, S., et al., Nanosilicon dot arrays with a bit pitch and a track pitch of 25 nm formed by electron-beam drawing and reactive ion etching for 1 Tbit/in.(2) storage. Applied Physics Letters, 2006. 89(22).

64. Chou, S.Y., P.R. Krauss, and P.J. Renstrom, IMPRINT OF SUB-25 NM VIAS AND TRENCHES IN POLYMERS. Applied Physics Letters, 1995. 67(21): p. 3114-3116.

65. Krauss, P.R. and S.Y. Chou, Nano-compact disks with 400 Gbit/in(2) storage density fabricated using nanoimprint lithography and read with proximal probe. Applied Physics Letters, 1997. 71(21): p. 3174-3176.

66. Vieu, C., et al., Electron beam lithography: resolution limits and applications. Applied Surface Science, 2000. 164: p. 111-117.

67. Hu, W.C., et al., Sub-10 nm electron beam lithography using cold development of poly(methylmethacrylate). Journal of Vacuum Science & Technology B, 2004. 22(4): p. 1711-1716.

68. Chang, T.H.P., PROXIMITY EFFECT IN ELECTRON-BEAM LITHOGRAPHY. Journal of Vacuum Science & Technology, 1975. 12(6): p. 1271-1275.

69. Ma, Y.S., G. Tsvid, and F. Cerrina, Line edge roughness of sub-100 nm dense and isolated features: Experimental study. Journal of Vacuum Science & Technology B, 2003. 21(6): p. 3124-3130.

70. Richter, H.J., et al., Recording on bit-patterned media at densities of 1 Tb/in(2) and beyond. Ieee Transactions on Magnetics, 2006. 42(10): p. 2255-2260.

71. Thomson, T., G. Hu, and B.D. Terris, Intrinsic distribution of magnetic anisotropy in thin films probed by patterned nanostructures. Physical Review Letters, 2006. 96(25).

72. Shaw, J.M., et al., Origins of switching field distributions in perpendicular magnetic nanodot arrays. Journal of Applied Physics, 2007. 101(2).

73. Kitade, Y., H. Komoriya, and T. Maruyama, Patterened media fabricated by lithography and argon-ion milling. Ieee Transactions on Magnetics, 2004. 40(4): p. 2516-2518.

74. Hattori, K., et al., Fabrication of discrete track perpendicular media for high recording density. Ieee Transactions on Magnetics, 2004. 40(4): p. 2510-2515.

75. Penaud, J., F. Fruleux, and E. Dubois, Transformation of hydrogen silsesquioxane properties with RIE plasma treatment for advanced multiple-gate MOSFETs. Applied Surface Science, 2006. 253(1): p. 395-399.

76. Kawamori, M., et al., Effect of oxygen plasma irradiation on hydrogen silsesquioxane nanopatterns replicated by room-temperature nanoimprinting. Japanese Journal of Applied Physics Part 1-Regular Papers Brief Communications & Review Papers, 2006. 45(11): p. 8994-8996.

77. Knigge, B., T. Suthar, and P. Baumgart, Friction, heat, and slider dynamics during thermal protrusion touchdown. Ieee Transactions on Magnetics, 2006. 42(10): p. 2510-2512.

78. Wachenschwanz, D., et al., Design of a manufacturable discrete track recording medium. Ieee Transactions on Magnetics, 2005. 41(2): p. 670-675.

79. Kamata, Y., et al., Ar ion milling process for fabricating CoCrPt patterned media using a self-assembled PS-PMMA diblock copolymer mask. Journal of Applied Physics, 2004. 95(11): p. 6705-6707.

80. Park, J., et al., Geometry transformation and alterations of periodically patterned Si nanotemplates by dry oxidation. Nanotechnology, 2009. 20(1).